

2016

## Novel Insight into the Role of LXR $\alpha$ in Metabolic Regulation via DNA Binding as a Heterodimer with PPAR $\alpha$ and as a Homodimer

Andrea M. Klingler  
*Wright State University*

Follow this and additional works at: [https://corescholar.libraries.wright.edu/etd\\_all](https://corescholar.libraries.wright.edu/etd_all)



Part of the [Molecular Biology Commons](#)

---

### Repository Citation

Klingler, Andrea M., "Novel Insight into the Role of LXR $\alpha$  in Metabolic Regulation via DNA Binding as a Heterodimer with PPAR $\alpha$  and as a Homodimer" (2016). *Browse all Theses and Dissertations*. 1573.  
[https://corescholar.libraries.wright.edu/etd\\_all/1573](https://corescholar.libraries.wright.edu/etd_all/1573)

This Thesis is brought to you for free and open access by the Theses and Dissertations at CORE Scholar. It has been accepted for inclusion in Browse all Theses and Dissertations by an authorized administrator of CORE Scholar. For more information, please contact [library-corescholar@wright.edu](mailto:library-corescholar@wright.edu).

**NOVEL INSIGHT INTO THE ROLE OF LXR $\alpha$  IN METABOLIC REGULATION  
VIA DNA BINDING AS A HETERODIMER WITH PPAR $\alpha$  AND AS A  
HOMODIMER**

A thesis submitted in partial fulfillment  
of the requirements for the degree of  
Master of Science

By

ANDREA M. KLINGLER

B.S. Biological Sciences, Wright State University, Dayton, OH 2013

2016

Wright State University

**WRIGHT STATE UNIVERSITY**  
**SCHOOL OF GRADUATE STUDIES**

Date, 2016

I HEREBY RECOMMEND THAT THE THESIS PREPARED UNDER MY SUPERVISION BY Andrea M. Klingler ENTITLED Novel Insight Into the Role of LXR $\alpha$  in Metabolic Regulation via DNA Binding as a Heterodimer with PPAR $\alpha$  and as a Homodimer BE ACCEPTED IN PARTIAL FULFILLMENT OF THE REQUIREMENTS FOR THE DEGREE OF Master of Science

\_\_\_\_\_  
S. Dean Rider, Jr., Ph.D.  
Thesis Director

\_\_\_\_\_  
Madhavi Kadakia, Ph.D., Chair  
Department of Biochemistry and Molecular Biology

Committee on Final Examination

\_\_\_\_\_  
S. Dean Rider, Jr., Ph.D.

\_\_\_\_\_  
Steven J. Berberich, Ph.D.

\_\_\_\_\_  
Lawrence J. Prochaska, Ph.D.

\_\_\_\_\_  
Michael Markey, Ph.D.

\_\_\_\_\_  
Robert E. W. Fyffe, Ph.D.  
Vice President for Research and Dean of the Graduate School

## ABSTRACT

Klingler, Andrea M. M.S., Department of Biochemistry and Molecular Biology, Wright State University, 2016. Novel Insight into the Role of LXR $\alpha$  in Metabolic Regulation via DNA Binding as a Heterodimer with PPAR $\alpha$  and as a Homodimer.

Liver X receptor  $\alpha$  (LXR $\alpha$ ) plays a critical role in the maintenance of energy homeostasis within a cell through tight transcriptional regulation of genes involved in metabolism of lipids, glucose, and cholesterol. Although LXR $\alpha$  has been established to function as a heterodimer with the retinoid X receptor  $\alpha$  (RXR $\alpha$ ), recent studies have determined that LXR $\alpha$  also interacts directly with peroxisome proliferator-activated receptor  $\alpha$  (PPAR $\alpha$ ). However, little is known regarding the functionality of this heterodimer, if any exists at all. This study determined that a heterodimer of PPAR $\alpha$  and LXR $\alpha$  is capable of binding to candidate response elements *in vitro* with high affinity by electrophoretic mobility shift assays and quenching of intrinsic protein fluorescence. Additionally, LXR $\alpha$  exhibited high affinity binding to DNA in the absence of a heterodimer partner, suggesting homodimeric interaction. Transactivation assays indicated that overexpression of PPAR $\alpha$  and LXR $\alpha$  significantly increased activity of the endogenous *APOA1* promoter, and overexpression of LXR $\alpha$  alone resulted in increased activity of all of the promoters tested, often even more so than LXR $\alpha$ /RXR $\alpha$ . These results provide new insight into the scope of metabolic regulation by LXR $\alpha$ , and raise important questions and considerations when targeting these proteins for treatment of metabolic disorders.

## TABLE OF CONTENTS

|   | <b>Page</b>  |
|---|--------------|
| <b>I. INTRODUCTION</b>  | <b>1-12</b>  |
| • Nuclear Receptors as Transcription Factors.....                         | 2            |
| • PPAR.....   | 5            |
| • LXR.....  | 8            |
| • PPAR and LXR: Cross-talk and Heterodimerization.....                    | 10           |
| <b>II. GOALS AND HYPOTHESES</b>   | <b>13</b>    |
| <b>III. MATERIALS AND METHODS</b>   | <b>14-28</b> |
| • Candidate Response Element Design.....                                  | 14           |
| • Protein Expression and Purification.....                                | 16           |
| • Electrophoretic Mobility Shift Assays.....                              | 17           |
| • Binding Assays.....   | 20           |
| • Candidate Response Element Validation and Location.....                 | 21           |
| • Gene Selection and Construction of Luciferase Reporter<br>Plasmids..... | 21           |
| • Transactivation Assays.....   | 28           |

|   |              |
|---|--------------|
| <b>IV. RESULTS</b>  | <b>29-55</b> |
| • PPAR $\alpha$ /LXR $\alpha$ binds candidate REs <i>in vitro</i> .....                                 | 29           |
| • PPAR $\alpha$ /LXR $\alpha$ and LXR $\alpha$ alone bind candidate REs with nanomolar<br>affinity..... | 34           |
| • Candidate REs occur naturally in the genome.....  | 43           |
| • PPAR $\alpha$ /LXR $\alpha$ and LXR $\alpha$ alone transactivate endogenous<br>promoters.....         | 45           |
| <br>  |              |
| <b>V. DISCUSSION</b>  | <b>56-64</b> |
| <b>VI. LIST OF ABBREVIATIONS</b>  | <b>65</b>    |
| <b>VII. REFERENCES</b>  | <b>66-75</b> |

## LIST OF FIGURES

| <b>Figure</b>   | <b>Page</b> |
|---|-------------|
| 1. Schematic representation of nuclear receptor structure and function.....                                     | 5           |
| 2. Construction of luciferase plasmid inserts for APOA1 and CXCR5.....  | 25          |
| 3. Construction of luciferase plasmid inserts for SULT2A1 and SREBP-1c (L4RE only).....                         | 26          |
| 4. Construction of luciferase plasmid inserts for TNFRSF4 and TNFRSF18.....                                     | 27          |
| 5. Preliminary EMSAs of PPAR $\alpha$ /LXR $\alpha$ with ABCG1 LXREs for buffer optimization.                   |             |
| (A) PPAR $\alpha$ /LXR $\alpha$ binding to ABCG1 LXRE with Buffer 1.....  | 31          |
| (B) PPAR $\alpha$ /LXR $\alpha$ binding to ABCG1 LXRE with Buffers 2, 3, and 4                                  | 31          |
| (C) PPAR $\alpha$ /LXR $\alpha$ binding to ABCG1 LXRE with Buffer 5.....  | 31          |
| 6. EMSA of PPAR $\alpha$ /LXR $\alpha$ with candidate response elements showing preference for DR4 element..... | 32          |
| 7. Supershift assay demonstrating presence of both PPAR $\alpha$ and LXR $\alpha$ in complex with DNA.....      | 33          |
| 8. Intrinsic fluorescence quenching of PPAR $\alpha$ upon titration with candidate REs.....                     | 35          |
| 9. Intrinsic fluorescence quenching of PPAR $\alpha$ upon titration with known                                  |             |

|   |           |
|---|-----------|
| REs.....  | 36        |
| <b>10. Intrinsic fluorescence quenching of LXR<math>\alpha</math> upon titration with candidate REs.....</b>  | <b>37</b> |
| <b>11. Intrinsic fluorescence quenching of LXR<math>\alpha</math> upon titration with known REs.....</b>  | <b>38</b> |
| <b>12. Intrinsic fluorescence quenching of PPAR<math>\alpha</math>/LXR<math>\alpha</math> upon titration with candidate REs.....</b>                        | <b>40</b> |
| <b>13. Intrinsic fluorescence quenching of PPAR<math>\alpha</math>/LXR<math>\alpha</math> upon titration with known REs.....</b>                            | <b>41</b> |
| <b>14. Plotting PPAR<math>\alpha</math>/LXR<math>\alpha</math> binding data on Hill coordinates suggests multiple binding sites.....</b>                    | <b>42</b> |
| <b>15. Genomic locations of the L4RE candidate response element relative to known PPAR<math>\alpha</math> and LXR<math>\alpha</math> binding sites.....</b> | <b>44</b> |
| <b>16. Western blot showing overexpression of transiently transfected PPAR<math>\alpha</math>, LXR<math>\alpha</math>, and RXR<math>\alpha</math> .....</b> | <b>46</b> |
| <b>17. Transactivation of APOA1.....</b>  | <b>48</b> |
| <b>18. Transactivation of CXCR5.....</b>  | <b>49</b> |
| <b>19. Transactivation of SULT2A1.....</b>  | <b>50</b> |
| <b>20. Transactivation of SREBP-1c (known PPRE and LXREs).....</b>  | <b>52</b> |
| <b>21. Transactivation of SREBP-1c (L4RE only) .....</b>  | <b>53</b> |
| <b>22. Transactivation of TNFRSF4.....</b>  | <b>54</b> |
| <b>23. Transactivation of TNFRSF18.....</b>   | <b>55</b> |



## LIST OF TABLES

| <b>Table</b> |  | <b>Page</b> |
|--------------|--|-------------|
| <b>1.</b>    | Sequences of candidate PPAR $\alpha$ /LXR $\alpha$ response elements.....  | 15          |
| <b>2.</b>    | Composition of binding buffers for EMSA reactions.....   | 19          |
| <b>3.</b>    | Primer sequences used in amplification of candidate target genes.....  | 24          |
| <b>4.</b>    | Binding affinities of PPAR $\alpha$ , LXR $\alpha$ , & PPAR $\alpha$ /LXR $\alpha$ for known &<br>candidate REs..... | 42          |

## **ACKNOWLEDGMENTS**

Firstly, I would like to dedicate this work to the memory of my late mentor, Dr. Heather Hostetler, without whose incredible guidance, encouragement, and belief in my worth as a scientist none of this would have been possible, and who I could never thank enough for giving me a chance when no one else would.

I would also like to sincerely thank my mentor, Dr. Dean Rider, for stepping in at a difficult time and giving freely of his time and expertise, and keeping me motivated to see this through.

I also thank my family, especially my husband, Blaine, and my son, Luke, for their unwavering support and encouragement through grad school, and everything they put up with along the way.

Finally, my fellow lab members and friends have been invaluable for help, encouragement, discussion, and anything else I might have needed from them, and for that, I thank them all immensely.

## I. INTRODUCTION

Energy homeostasis is maintained in the body through tight regulation of the biochemical processes involved in metabolism. The importance of such regulation is evident in the instance of its failure, as is seen in metabolic disorders. As of 2012, 2.7% of US adults had been affected by cerebrovascular disease or stroke, 13.4% were affected by high cholesterol, 11.3% with heart disease, and 32.5% with hypertension. In addition, 11.9% of US adults were affected with diabetes as of 2010, and, as of 2012, 69% of US adults were overweight or obese, a condition which has been shown to contribute to the likelihood of the previously mentioned diseases and conditions. Since these conditions are among the top 10 causes of death in the United States, understanding the mechanisms behind the regulation of metabolic processes involved is of the utmost importance. Focus in this interest has been turned toward the proteins, known as nuclear receptors, which control elements of numerous pathways of metabolism, especially those which regulate levels of glucose, intracellular lipids, and cholesterol by acting as transcription factors and altering gene expression to achieve the desired effect. By teasing apart the regulatory mechanisms involved, it will be possible to achieve maintenance and/or prevention of these conditions more readily.

## **Nuclear Receptors as Transcription Factors**

Nuclear receptors are ligand-activated transcription factors that alter the expression of genes in order to regulate cellular processes. They are distinct from membrane-bound receptors in that they are located in the interior of the cell, and thus are activated by small, hydrophobic molecules that are able to diffuse through the membrane into the cytosol, such as steroid hormones or other lipids. Nuclear receptors respond to changes in cellular metabolic requirements by binding a consensus sequence in genomic DNA in order to initiate transcription of target genes. To date, 48 individual nuclear receptor genes have been identified in the human genome, and they are further classified into six subfamilies based on sequence homology: the NR1 subfamily proteins are similar to the thyroid hormone receptor (TR), which includes the peroxisome proliferator-activated receptors (PPARs), the liver X receptors (LXRs), and the retinoic acid receptors (RARs). The NR2 subfamily is comprised of the retinoid X receptors (RXRs) and other receptors with similar properties, including hepatic nuclear factor 4 (HNF4). Hormone receptors such as the estrogen receptor (ER), androgen receptor (AR), and progesterone receptor (PR) are grouped into the NR3 subfamily, with the remaining subfamilies having relatively few members of note. Additionally, identified receptors which cannot be easily classified are grouped into subfamily NR0. One example is the small heterodimer partner (SHP), which lacks a domain to bind DNA. Receptors are further classified into one of four types based on mechanistic action properties and their subcellular localization in relation to ligand binding, DNA binding and dimerization properties: Type I nuclear receptors include members of the NR3 subfamily, which bind their respective ligands and

form homodimers in the cytoplasm before translocating into the nucleus and then activate transcription at inverted repeat sequences known as hormone response elements (HRE). Type II nuclear receptors, which include members of the NR1 subfamily as well as RXR, are localized in the nucleus independently of ligand binding and bind direct repeat sequences as heterodimers. It is also noteworthy that the constitutive androstane receptor (CAR), a member of the NR1 subfamily, is ligand-independent and constitutively active. Type III receptors are similar to Type II in that they bind direct repeat sequences, but they have the requirement of forming homodimers, and include members of the NR2 subfamily, such as RXR. Finally, Type IV receptors bind only a single RE half-site, and are the only nuclear receptors that bind DNA as a monomer, although some are also capable of binding as a dimer.

Nuclear receptors exhibit a characteristic modular structure comprised of five domains linked to their function as ligand-activated, DNA-binding proteins. The N-terminal A/B domain of nuclear receptors is highly variable among family members, and has no three-dimensional crystal structure. This region has, nevertheless, been shown to be important as a site of post-translational modification [1] and carries out the protein's ligand-independent transcriptional activation function [2]. DNA binding occurs at the highly conserved C region, or DNA-binding domain (DBD). This domain consists of two zinc-finger motifs, which exact the two functions necessary for successful DNA binding and transcriptional activation: recognition of and binding to RE sequences, and facilitation of dimerization between receptor partners. Located within the amino-terminal zinc finger is a region known as the proximal- or P-box, which consists of cysteine residues bonded to a zinc ion and surrounding residues, the sequence of which confers

response element sequence specificity. The carboxy-terminal zinc finger contains the distal-, or D-box region, which is involved in receptor dimerization. Separating the DBD from the ligand-binding domain is a flexible, less-conserved hinge region, which contains the receptor's nuclear localization signal and allows for conformational changes in the surrounding domains. Activating ligands bind their respective receptor at the ligand-binding domain (LBD), which consists of alpha-helices and forms a hydrophobic "pocket" in which the ligand may fit. The size of the ligand binding pocket, intuitively, varies from receptor to receptor in order to accommodate each protein's preferred ligand; for example, the ligand binding pocket of PPAR $\alpha$  has a volume of 1177 Å<sup>3</sup> [3], while that of LXR $\alpha$  is 700-800 Å<sup>3</sup> [4]. Additionally, the ligand binding domain contains a dimerization interface and the ligand-dependent activation function. The C-terminal region of nuclear receptors is also a site of post-translational modification, and it acts as a "lid" over the ligand binding pocket upon ligand entry and binding.

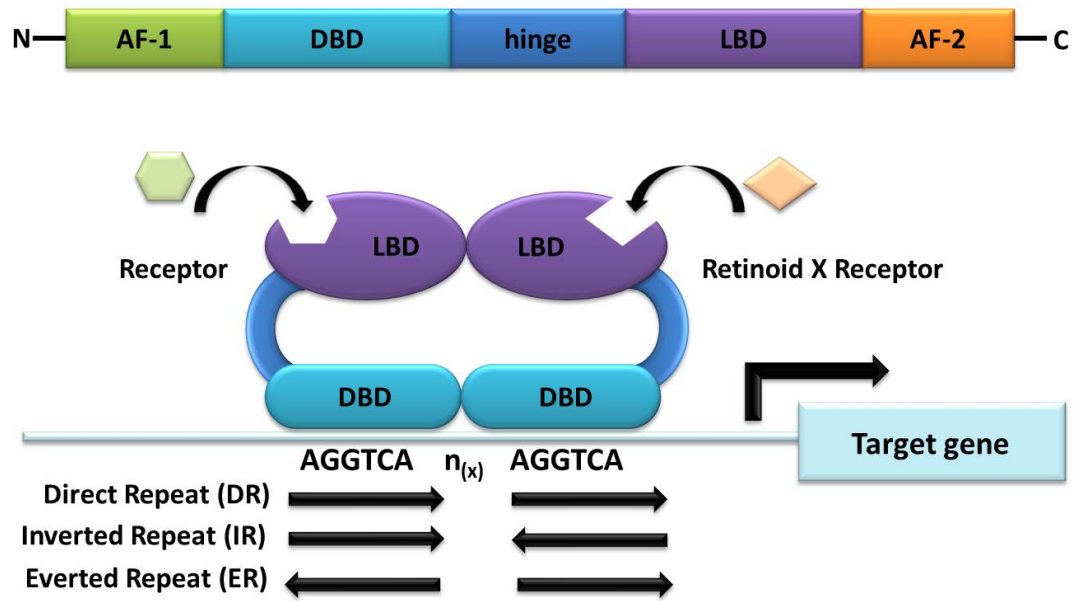


**Figure 1. Schematic representation of nuclear receptor structure and function.** Nuclear receptor proteins exhibit a characteristic modular structure consisting of five domains: N-terminal AF-1, DNA-binding domain (DBD), a flexible hinge region, ligand binding domain (LBD), and the C-terminal AF-2 domain. Type II receptors form permissive heterodimers with RXR $\alpha$ , and the DNA binding domains bind the half-sites of a response element to activate or repress transcription of target genes.

As previously mentioned, nuclear receptors alter gene expression by recognizing and binding their respective REs, which typically consist of hexameric repeats of direct, inverted, or everted orientation (DR $x$ , IR $x$ , or ER $x$ , respectively). The nucleotide hexamers are separated by a small sequence of spacer nucleotides, generally 1 to 10 nucleotides in length and of variable sequence. The significance of the spacer nucleotides is not entirely clear. Further, nuclear receptors can use response elements to activate transcription regardless of whether the sequence is on the plus or minus strand. Response elements are located throughout the genome, primarily in promoter regions or other areas upstream of the coding sequences, although response elements have been characterized in

intronic regions as well. In particular, the ABCA1 gene has been shown to have a response element for LXR $\alpha$  in the promoter region, as well as another functional promoter and response element in the first intron. However, the role of this response element in eliciting a physiological effect was not determined [5]. Since extensive cross-talk exists between regulatory proteins, genes may have response elements for many different nuclear receptors. The hierarchy of control regarding genes containing multiple response elements is not necessarily the result of distance from the promoter, but is in fact based on several factors, such as tissue-specific expression of receptors, concentration of receptors and their respective ligands, and relative binding affinities. A well-known example of this, and one of particular relevance to this study, is the promoter region of SREBF1, which codes for the sterol regulatory element binding protein (SREBP-1c). This section contains two LXR response elements (LXRE) in addition to a PPAR response element (PPRE). Activation of its RE by LXR $\alpha$  results in upregulation of the gene, while PPAR $\alpha$  activation represses SREBP-1c expression.

## **PPAR**

Peroxisome proliferator-activated receptors (PPARs) are a group of nuclear receptors that belong to the NR1 subfamily, which also includes the vitamin D receptor (VDR), farnesoid X receptor (FXR), and the RAR-related orphan receptor (ROR). Three isoforms of PPAR have been identified, which are coded for by separate genes: PPAR $\alpha$ , PPAR $\beta/\delta$ , and PPAR $\gamma$ . Owing to their tissue specificity, the three isoforms of PPAR bind distinct ligands and have roles in distinct processes. PPAR $\alpha$ , cloned in 1990 [6] and



the first of the isoforms identified, is primarily found in the liver, heart, kidney, adrenal glands, and other tissues, and is a regulator of the body's response to fasting, primarily as pertains to oxidation of lipids. PPAR $\delta$  is ubiquitously expressed, and activated by synthetic compound GW501516, and also functions as a regulator of fatty acid oxidation, as well as electron transport chain uncoupling and thermogenesis. PPAR $\gamma$  is abundant in white adipose tissue as well as in macrophages, and its ligands include thiazolidinediones, a class of drugs used to increase insulin sensitivity in diabetic patients. The receptor functions in adipose tissue to regulate genes involved in adipogenesis and cell differentiation. As the predominant isoform present in highly metabolic tissues and a critical player in the body's regulation of energy homeostasis, PPAR $\alpha$  will be the focus of this study.

A type II nuclear receptor, PPAR $\alpha$  forms a permissive heterodimer with the retinoid X receptor alpha (RXR $\alpha$ ) to bind a direct-repeat 1 motif (DR1) in order to initiate transcription of its target genes. The nucleotide sequence of identified PPREs can be quite degenerate from the consensus AGGTCA $n$ AGGTCA sequence, although PPAR $\alpha$  is not quite as promiscuous as some other receptors, such as RXR $\alpha$ . Even so, PPAR $\alpha$  has been observed binding to a known PXR/CAR binding site near the gene encoding cytochrome p450 (CYP2C8), which follows a DR-4 motif [7]. As previously mentioned, PPAR $\alpha$  targets are generally involved in pathways comprising the body's response to fasting, in particular the breakdown of fats for energy. Long-chain fatty acids (LCFA) and their thioester derivatives (LCFA-CoA) serve as high affinity endogenous ligands for PPAR $\alpha$  [8], and as such the receptor is responsible for direct regulation of many key

enzymes in mitochondrial, microsomal and peroxisomal fatty acid oxidation, such as acyl-CoA oxidase (ACOX1). HMG-CoA synthase (HMGCS2), which is responsible for a step in the process of converting fatty acids to ketone bodies in order to be transported elsewhere to be used for energy, is another target. PPAR $\alpha$  and its agonists have also been linked to regulation of genes involved in the transport of fatty acids, such as carnitine palmitoyl transferase (CPT1), which aids in the transport of fatty acids into the mitochondria for oxidation, as well as liver-type fatty acid binding protein (L-FABP), with which PPAR $\alpha$  also interacts directly [9]. In addition to increasing expression of genes involved in lipid catabolism, PPAR $\alpha$  also decreases expression of genes responsible for the synthesis of fatty acids, such as fatty acid synthase (FAS)[10] and acetyl-CoA carboxylase (ACC)[11], indirectly through repression of SREBP-1c[12]. PPAR $\alpha$  also plays a role in regulation of cholesterol metabolism, inducing breakdown of lipoproteins through lipoprotein lipase (LPL)[13] and increase high density lipoproteins (HDL) through direct control of major components such as apolipoprotein AI [14], and in glucose metabolism through pyruvate dehydrogenase kinase 4 (PDK4)[15]. Additionally, PPAR $\alpha$  functions in an anti-inflammatory capacity through negative cross-talk with pro-inflammatory transcription factors [16] and through binding and inducing breakdown of leukotriene B4 [17], a derivative of arachidonic acid involved in inflammation.

Many prevalent metabolic disorders arise from dysregulation of fatty acid and glucose metabolism, and are characterized by increased levels of free fatty acids, cholesterol, and inflammation. Since PPAR $\alpha$  is a prominent regulator of fatty acid metabolism as well as a factor in negative regulation of inflammation, it is implicated in

many such disease processes, in addition to being an attractive therapeutic target. A number of synthetic and endogenous ligands have been identified for PPAR $\alpha$ , beginning with compounds known as peroxisome proliferators that are carcinogenic to rodents and led to the receptor's initial identification. As an important regulator of lipid metabolism, PPAR $\alpha$  is the target of a class of hypolipidemic drugs known as fibrates, as well as the compound Wy-14,643, which are used to treat cardiovascular disease by correcting cholesterol and triglyceride levels. Additionally, a number of naturally occurring lipids have been shown to bind PPAR $\alpha$  *in vitro* and affect transactivation in cells. The relatively large size allows the binding pocket to accommodate a diverse range of lipid conformations, from long-chain fatty acids such as palmitic (C16:0) and arachidonic (C20:4) acids, branched-chain fatty acids, and much larger fatty acyl-CoA thioesters, as well as those of very long-chain fatty acids [8, 18]. In fact, PPAR $\alpha$  binds the CoA thioesters of many saturated long-chain and very long-chain fatty acids with higher affinity than the respective free fatty acids. Moreover, PPAR $\alpha$  has been shown to bind non-lipid molecules as well; specifically, sugars, such as glucose [19].

## **LXR**

Liver X receptor alpha (LXR $\alpha$ ) is also a member of the NR1 subfamily, and, similarly to PPAR $\alpha$ , is predominantly expressed in the liver, kidney, lung, intestine, macrophages and adipose tissue. A second isoform, LXR $\beta$ , has significant sequence homology to LXR $\alpha$ , but is expressed ubiquitously. Like PPAR $\alpha$ , LXR $\alpha$  is a type II nuclear receptor and also forms heterodimers with RXR $\alpha$ . However, the LXR $\alpha$ /RXR $\alpha$

heterodimer binds a direct-repeat 4 (DR4) response element known as a liver X receptor response element (LXRE), as opposed to the DR1 that is bound by PPAR $\alpha$ . The sequence specificity of LXREs is greater than that of PPREs, but some degeneracy is still observed. The physiological role of LXR $\alpha$ , like that of PPAR $\alpha$ , has been elucidated as that of an important nutrient sensor and regulator of metabolic processes, although LXR $\alpha$  modulates pathways which often work in the opposite direction of those involving PPAR $\alpha$ , mainly cholesterol metabolism and fatty acid synthesis. Highly characterized LXR $\alpha$  target genes include sterol regulatory element-binding protein 1c (SREBP-1c) [20], which is a transcription factor responsible for regulating levels of fatty acids and cholesterol in the cell, and cholesterol transporters such as the ATP-binding cassettes A1, G1, G5, and G8 [21-23]. Additionally, LXR $\alpha$  is also a known regulator of apolipoprotein E (ApoE), carbohydrate response element-binding protein (ChREBP), and FAS. Accordingly, oxidized cholesterol such as 22(R)-hydroxycholesterol and other oxysterols have been shown to function as LXR $\alpha$  ligands. Further, LXR $\alpha$  has been identified as a glucose sensor [24], similarly to PPAR $\alpha$ , and has an important anti-inflammatory role in preventing macrophage foam cell formation and decreasing atherogenesis. Thus, LXR $\alpha$  has been strongly implicated in disease states involving excess fats and cholesterol, such as hypercholesterolemia, atherosclerosis, cardiovascular disease, and hyperlipidemia. Genetic variation in the receptor is linked with increased risk of metabolic issues. Of particular note is a single nucleotide polymorphism (SNP) at -1830 bp that, in conjunction with mutations at -840 bp and -115 bp from the ATG start codon, is associated with increased risk of ischemic vascular disease [25]. In addition, risk of developing symptoms of metabolic syndrome is also influenced by genetic

variation in LXR $\alpha$  [26]. LXR $\alpha$  knockouts have resulted in hepatomegaly, increased atherogenesis and macrophage lipid accumulation, as well as symptoms resembling Tangier disease, which is related to the LXR $\alpha$  target gene ABCA1. As previously mentioned, LXR $\alpha$  is an important regulator of SREBP-1c, which is important in regulating cell cholesterol and fatty acid levels. This poses a problem when considering LXR $\alpha$  as a therapeutic target: while LXR $\alpha$  activation does decrease atherogenesis and increase cholesterol efflux, it also results in increased triglycerides. It is for this reason that, despite showing potential to alleviate symptoms of metabolic disorders, drugs targeting LXR $\alpha$  have not been approved for use.

### **PPAR and LXR: Cross-talk and Heterodimerization**

Previous studies have indicated that significant cross-talk exists between the pathways regulated by PPAR $\alpha$  and LXR $\alpha$ . Many genes upregulated by LXR $\alpha$  are in turn downregulated by PPAR $\alpha$ , and vice versa. A prime example of this is that LXR $\alpha$  has been shown to repress PPAR $\alpha$ /RXR $\alpha$  activation of ACOX, while conversely, PPAR $\alpha$  represses LXR $\alpha$ /RXR $\alpha$ -mediated activation of SREBP-1c [27-29]. Agonists for PPAR $\alpha$ , LXR $\alpha$ , and RXR $\alpha$  have been shown to have overlapping transcriptional programs as well, [30]. Further, a 2012 study by Boergesen et al.[31] observed an overlap of binding sites occupied by PPAR $\alpha$  and LXR $\alpha$  in mouse liver. PPAR and LXR have been suggested to bind DNA in areas where a PPRE and an LXRE overlap, as was observed with the CYP7A1 gene [32], and further study by the same group determined PPAR $\alpha$ /LXR $\alpha$  may be responsible for repression of CYP7A1 in humans, rather than LXR $\alpha$ /RXR $\alpha$  as is seen

in mice [33]. Despite their canonical mechanism involving heterodimerization with RXR $\alpha$ , interest in the field has recently turned toward direct interaction between PPAR $\alpha$  and LXR $\alpha$  themselves. A study by Miyata et al. using human and mouse protein suggested interaction through two-hybrid screening and *in vitro* protein binding assays [34]. Also, the kinetics of interaction between the LBD of PPAR $\alpha$  and LXR $\alpha$  have been investigated through surface plasmon resonance (SPR) and molecular dynamics simulations (MD) [35], concluding that the LBDs of the proteins are capable of interaction. Despite this, these and other studies have concluded that the heterodimerization of PPAR $\alpha$  and LXR $\alpha$  results in a nonfunctional complex that is incapable of binding DNA. More recently, it has come to light that human and mouse PPAR $\alpha$  behave differently in terms of ligand binding [36], and that it is necessary to examine this interaction using full-length, human proteins to properly elucidate its function. Such studies have been completed, showing that full-length, human PPAR $\alpha$  and LXR $\alpha$  interact *in vitro* through fluorescent binding assays and circular dichroism spectroscopy, and *in vivo* through transactivation assays and co-immunoprecipitation [37]. More importantly, electrophoretic mobility shift assays determined that these proteins were able to bind DNA *in vitro*, suggesting that not only is the heterodimer capable of binding DNA, it may indeed be functional. Although none of the genes tested in the aforementioned re-ChIP experiments, such as SREBP-1c and HMGCS2, were bound simultaneously by both proteins [31], this does not rule out the possibility that a heterodimer could bind at these, or other, genomic locations, and possibly serve a regulatory function itself.

## II. GOALS AND HYPOTHESES

The goal of this study is to examine if full-length, human PPAR $\alpha$ /LXR $\alpha$  heterodimers to act in a functional capacity and regulate gene expression through high affinity binding to DNA. Furthermore, since a response element for PPAR $\alpha$ /LXR $\alpha$  heterodimers has not been previously identified, this study aims to establish whether PPAR $\alpha$ /LXR $\alpha$  heterodimers bind a specific type of response element, and if that response element occurs naturally in the human genome.

To that end, the specific aim of this thesis is that PPAR $\alpha$ /LXR $\alpha$  binds a novel DNA sequence as a heterodimer with high affinity, and that the sequence occurs in genomic locations near relevant promoters that result in statistically significant transactivation upon binding by PPAR $\alpha$ /LXR $\alpha$ .

### III. MATERIALS AND METHODS

#### Candidate Response Element Design

It is well known that PPAR $\alpha$  and LXR $\alpha$ , when in complex with RXR $\alpha$ , bind a DR1 and DR4 response element, respectively. However, there is no guarantee that the PPAR $\alpha$ /LXR $\alpha$  heterodimer follows the binding characteristics of either individual protein, or that the AGGTCA\_AGGTCA sequence is also the ideal site for this heterodimer to bind. Miyata et al. examined PPAR $\alpha$ /LXR $\alpha$  binding to idealized sequences in the form of DR0-DR5 response elements by electrophoretic mobility shift [34], but none was observed with the hexameric sequences used. Thus, this study examined consensus sequences for known PPREs [38] and LXREs [39] for the most commonly observed half-sites, and those half-sites were used to construct candidate PPAR $\alpha$ /LXR $\alpha$  response elements whose half-sites corresponded to those of a PPRE (P), an LXRE (L), or a hybrid of PPRE and LXRE (H). To determine the influence of the number of nucleotides separating the half-sites, sequences separated by 1, 2, 3, or 4 nucleotides were designed. Single-stranded oligonucleotide primers (Table 1) were purchased from IDT (Coralville, IA) and dissolved to 1  $\mu\text{g}/\mu\text{l}$  stock solution in 1X TE. The forward and reverse primers were mixed in annealing buffer (10mM Tris, pH 8.0, 1mM EDTA, 50mM NaCl) and incubated at 95°C in a dry bath for 5 min. The aluminum block was then removed from heat and the oligonucleotide solutions were allowed to



return to room temperature over 2-3 hours. Concentration was determined from absorbance measurements at 260 nm using a Nanodrop spectrophotometer, and purity was assessed from ratios of absorbance measured at 260 nm/280nm and 260 nm/230 nm.

| <b>Element</b> | <b>Sequence</b>                                     |
|----------------|---|
| <b>P1RE</b>    | 5'- gatcttc <u>AGGGCA</u> a <u>AGGTCA</u> gg -3'    |
| <b>P2RE</b>    | 5'- gatcttc <u>AGGGCA</u> ag <u>AGGTCA</u> gg -3'   |
| <b>P3RE</b>    | 5'- gatcttc <u>AGGGCA</u> agc <u>AGGTCA</u> gg -3'  |
| <b>P4RE</b>    | 5'- gatcttc <u>AGGGCA</u> agct <u>AGGTCA</u> gg -3' |
| <b>L1RE</b>    | 5'- gatcttc <u>GGATCA</u> c <u>AGGTCA</u> gg -3'    |
| <b>L2RE</b>    | 5'- gatcttc <u>GGATCA</u> cc <u>AGGTCA</u> gg -3'   |
| <b>L3RE</b>    | 5'- gatcttc <u>GGATCA</u> cct <u>AGGTCA</u> gg -3'  |
| <b>L4RE</b>    | 5'- gatcttc <u>GGATCA</u> cctg <u>AGGTCA</u> gg -3' |
| <b>H1RE</b>    | 5'- gatcttc <u>AGGGCA</u> c <u>GGATCA</u> gg -3'    |
| <b>H2RE</b>    | 5'- gatcttc <u>AGGGCA</u> cc <u>GGATCA</u> gg -3'   |
| <b>H3RE</b>    | 5'- gatcttc <u>AGGGCA</u> cct <u>GGATCA</u> gg -3'  |
| <b>H4RE</b>    | 5'- gatcttc <u>AGGGCA</u> cctg <u>GGATCA</u> gg -3' |

**Table 1. Sequences of Candidate PPAR $\alpha$ /LXR $\alpha$  Response Elements.** Oligonucleotide primers were used for *in vitro* assessment of protein-DNA interactions. Half-sites are presented in underlined capital letters, while spacer nucleotides and extraneous 5' and 3' sequence are in lower case.

## **Protein Expression and Purification**

Full-length, recombinant human PPAR $\alpha$ , LXR $\alpha$ , and RXR $\alpha$  were expressed and purified using plasmids constructed in the laboratory [37], which contained the cDNA for the appropriate protein inserted into the pGEX-6-P3 vector for expression in bacterial cells. These proteins were expressed with an N-terminal glutathione S transferase (GST) affinity tag separated from the start codon by a 6X histidine tag to aid in purification. Expression plasmids were transformed into Rosetta 2 cells (Novagen, Philadelphia, PA) and grown overnight in 100 ml (for PPAR $\alpha$  and RXR $\alpha$ ) or 40 ml (for LXR $\alpha$ ) Luria Bertani (LB) broth media supplemented with 0.1mg/ml ampicillin, 0.2 mg/ml chloramphenicol, and 10% glucose at 30°C and 200 rpm. Overnight cultures were subcultured into 1 L prewarmed LB the following day and grown at 37°C until the desired OD600 (1-1.5) was reached, approximately 2-3 hours. At this point, 0.1 M IPTG was added to the cultures to induce protein expression, and incubated at 16°C for a further 4 hours. Following this, cells were pelleted in an Avanti-J26 XPI centrifuge at 8500 rpm for 10 minutes at 4°C. 100mM PMSF was added to each pellet to inhibit proteolysis, and the pellets were stored at -80°C until purification.

Pellets were resuspended in 10 ml 2X L&C buffer (40mM Tris, pH 8.0, 0.35mM NaCl, and 20% glycerol), 1mM DTT, 2mM EDTA, and 10 ml EDTA-free protease inhibitor cocktail (SIGMAFAST, Sigma-Aldrich, St. Louis, MO) dissolved in 2X L&C buffer. Cell membranes were disrupted by sonication at 50% amplitude for six 30 second intervals, with 30 seconds between each. Following sonication, the cell suspension was

centrifuged at 10,000 rpm for 20 minutes to remove cell debris and produce a cleared cell lysate, which was then circulated on 1 mL GST affinity columns with a flow rate of 0.1 ml per minute at 4°C.

Following complete circulation of the cleared lysates, the columns were washed once with 2 ml 1X L&C buffer (20mM Tris, pH 8.0, 0.175mM NaCl, and 10% glycerol), once with 5 ml 2X L&C buffer containing 10mM ATP and 50mM MgCl<sub>2</sub>, and lastly with 10 ml 1X L&C buffer containing 1mM DTT and 2mM EDTA to ensure removal of all but tagged, bound protein from the column. On-column cleavage of the His-GST tag was accomplished by circulating 1 ml 1X L&C buffer containing 1mM DTT, 2mM EDTA, and 120 µg PreScission protease (GE Healthcare Life Sciences, Pittsburgh, PA) for 4 hours, and untagged protein collected in 1 ml eluates until all protein was removed. Concentration of eluates was estimated by Bradford assay, and protein purity assessed by SDS-PAGE followed by Coomassie blue staining, and aliquots were stored at -80°C until use.

### **Electrophoretic Mobility Shift Assays**

Two hundred ng of each purified protein were incubated in binding buffer with 40 ng double-stranded oligonucleotide for 30 minutes at room temperature, then cross-linked by UV irradiation (Stratagene, San Diego, CA) at 120mJ/cm<sup>2</sup>. Samples were then mixed with 6X gel loading buffer included in the Molecular Probes kit (Invitrogen, Carlsbad, CA) and protein-DNA complexes were resolved on 6% native polyacrylamide gels in

0.5X TBE buffer with a 100 bp DNA ladder (Invitrogen, Carlsbad, CA) and a protein ladder (BioRad, Hercules, CA). To visualize protein-DNA complexes, gels were stained with SYBR green (diluted to 1X in TBE buffer) for 20 minutes while protected from light, rinsed, and imaged on a Fujifilm LAS-3000 cooled charge-coupled device camera. Gels were then stained overnight in SYPRO Ruby, destained in destaining solution (10% methanol, 7.5% acetic acid), and imaged. Relative band intensities were quantified as mean 16-bit grayscale density in ImageJ (<https://imagej.nih.gov/ij/download.html>). Since PPAR $\alpha$ /LXR $\alpha$  binding has not been previously observed in fluorescent EMSA experiments, several compositions of binding buffer were examined to determine optimal conditions for the reaction (see Table 2 [22, 40, 41]). Buffers were prepared as 5X solutions, with the final concentration in the binding reaction being 1X. Similar experiments were conducted with PPAR $\alpha$  only, LXR $\alpha$  only, RXR $\alpha$  only, PPAR $\alpha$ /RXR $\alpha$ , and LXR $\alpha$ /RXR $\alpha$ . To confirm both PPAR $\alpha$  and LXR $\alpha$  were present in the shifted complexes, supershift assays were carried out by adding 1  $\mu$ g of anti-PPAR $\alpha$  (sc-1985X, Santa Cruz Biotechnology, Santa Cruz, CA) or anti-LXR $\alpha$  (PA1-9066, Pierce) antibody after cross-linking and allowing the mixture to equilibrate for 15 minutes. Supershifted complexes were resolved on 4% non-denaturing polyacrylamide gels, stained and imaged as described.

| <b>1</b>   | <b>2</b>   | <b>3</b>  | <b>4</b>   | <b>5</b>   |
|--|--|---|--|--|
| 20mM HEPES<br>75mM KCl<br>2mM DTT<br>7.5% Glycerol<br>0.1% NP-40 | 20mM Tris<br>(pH 8.0)<br>60mM KCl<br>1.3mM MgCl <sub>2</sub><br>0.2mM EDTA<br>0.5mM DTT<br>10% Glycerol<br>3% Ficoll | 10mM Tris<br>(pH 7.5)<br>50mM KCl<br>2.5mM MgCl <sub>2</sub><br>0.05mM<br>EDTA<br>1mM DTT<br>8.5% Glycerol<br>0.1% Triton X-<br>100 | 20mM Tris<br>(pH 8.0)<br>60mM KCl<br>1.3mM MgCl <sub>2</sub><br>0.2mM EDTA<br>0.5mM DTT<br>10% Glycerol<br>0.6% Ficoll | 10mM Tris<br>(pH 7.5)<br>50mM KCl<br>2.5mM MgCl <sub>2</sub><br>0.05mM<br>EDTA<br>1mM DTT<br>8.5% Glycerol |

**Table 2. Composition of binding buffers for EMSA reactions.** Concentrations given are for 1X solutions. Buffers were prepared as 5X solutions and diluted as necessary.

## **Binding assays**

Fifty nM each of purified recombinant PPAR $\alpha$  and LXR $\alpha$  were mixed in phosphate buffered saline (PBS) and titrated against increasing concentrations (0-200 nM) of annealed double-stranded oligonucleotide (P4RE, L4RE, H4RE, ACOX PPRE, or SREBP-1c LXRE). After 3 minute equilibration, quenching of intrinsic aromatic amino acid fluorescence at 24°C was measured by monitoring emission spectra (310 nm – 370 nm) using an excitation wavelength of 280 nm obtained on a PC1 photon counting spectrofluorometer (ISS, Champaign, IL). Changes in maximal fluorescence intensity following subtraction of PBS blank were plotted against oligonucleotide concentration. Binding affinity was estimated by nonlinear regression analysis using the ligand binding function of Sigma Plot (SPSS, Chicago, IL). Subsequent experiments were repeated using titrations up to 40 nM oligonucleotide. Similar experiments were also done to assess the binding affinities for PPAR $\alpha$  and LXR $\alpha$  individually, using 100 nM protein concentration.

## Candidate Response Element Validation and Location

Available data from PPAR $\alpha$  and LXR $\alpha$  ChIP-seq experiments was obtained from supplemental files from [31] in BED format and checked for overlap using Microsoft Excel and bedtools (<https://github.com/arq5x/bedtools2/releases>). Local BLAST ([https://blast.ncbi.nlm.nih.gov/Blast.cgi?PAGE\\_TYPE=BlastDocs&DOC\\_TYPE=Download](https://blast.ncbi.nlm.nih.gov/Blast.cgi?PAGE_TYPE=BlastDocs&DOC_TYPE=Download)) was then used to align the resulting overlapping sites to the Hg19 human genome assembly. Additionally, LXR $\alpha$  ChIP-seq data from a monocyte-induced macrophage cell line [42] was obtained. Finally, local BLAST (optimized for short nucleotide sequences) was used to locate instances of the P4RE, L4RE, and H4RE candidate response elements in the genome, with word size set to 16 and percent identity set to 100. Output files in BED format for ChIP-seq data sets and RE searches were then used to generate tracks using Integrated Genome Browser (<http://bioviz.org/igb/download.html>).

## Gene Selection and Construction of Luciferase Reporter Plasmids

NCBI BLAST was used to search the human genome for occurrences of the P4RE, L4RE, and H4RE sequences, and exact matches located within 5kb of an identified promoter [43,44] were considered. Three known targets of PPAR $\alpha$  and LXR $\alpha$  were chosen for further study: apolipoprotein A1 (*APOA1*), a component of high-density lipoproteins known to be regulated by PPAR $\alpha$  and LXR $\alpha$  [14,45]; cytosolic sulfotransferase 2A1 (*SULT2A1*), involved in sulfation of steroids (such as cholesterol) and bile acids in order to facilitate excretion and known to be regulated by PPAR $\alpha$  and LXR $\alpha$  [46,47]; and sterol regulatory element binding protein 1c (*SREBP-1c*). Three

potential novel targets were chosen based on expression of both PPAR $\alpha$  and LXR $\alpha$  in B and T lymphocytes [48-51] and the possibility that PPAR $\alpha$ /LXR $\alpha$  heterodimers regulate a distinct subset of genes (as opposed to those already associated with either protein). The three were: C-X-C chemokine receptor 5 (*CXCR5* or BLR1), involved in B cell migration and Burkitt's lymphoma; tumor necrosis factor superfamily member 4 (*TNFRSF4*, also known as OX40), and tumor necrosis factor receptor superfamily member 18 or glucocorticoid-induced TNF receptor (*TNFRSF18* or GITR). Separate fragments containing the L4RE and the promoters of *APOA1*, *SULT2A1*, and *CXCR5* were amplified by polymerase chain reaction from genomic DNA isolated from HepG2 cells using primers indicated in Table 3. Fragments were cloned separately into the pGEM-T easy vector and subsequently transferred as one insert into the *KpnI-SacI* (for *APOA1* and *SULT2A1*) or *BglII-XhoI* (for *CXCR5*) sites of the luciferase reporter plasmid pGL4.17 to generate *APOA1*-pGL4.17, *SULT2A1*-pGL4.17, and *CXCR5*-pGL4.17. *TNFRSF4* was amplified using the indicated primers as a single 712 bp fragment containing both the L4RE and the promoter and cloned into the pGEM-T easy vector, then transferred to the *KpnI-SacI* sites of pGL4.17 to generate *TNFRSF4*-pGL4.17. *TNFRSF18* was amplified as a single 1321 bp fragment containing both the L4RE and the promoter using the indicated primers and cloned into the pGEM-T easy vector before being transferred to the *KpnI-XhoI* sites of pGL4.17 to produce *TNFRSF18*-pGL4.17. The promoter for SREBP-1c with and without known PPRE and LXRE sequences had been previously cloned into pGL4.17. A short fragment (355 bp) containing only the L4RE was amplified using the indicated primers and cloned into pGEM-T before being inserted into the existing



SREBP-1c-pGL4.17 plasmid using the *KpnI-EcoRI* sites to produce SREBP-1cShort-pGL4.17. Plasmids were verified by DNA sequencing performed by Retrogen.

| Gene     |               | Primer Sequences (forward and reverse)   |
|----------|---------------|--|
| APOA1    | L4RE          | 5'- <u>tggtacc</u> AGAGGTCTCCCAGGCTAAGG - 3'<br>5' - <u>cgaattc</u> GCAGTAACCTCTGCCTCCTG - 3'    |
|          | Promoter      | 5' - <u>tgaattc</u> GGGGAGGGGAGTGAAGTAGT -3'<br>5' - <u>cgagctc</u> GTGAGGAGAAGGGCACAGAG -3'     |
| CXCR5    | L4RE          | 5' - <u>ttaggtacc</u> GGGGCAGGGATATTGAGAAT -3'<br>5' - <u>cctcatatg</u> GGGTTTCTCCATGTTGGTCA -3' |
|          | Promoter      | 5' - <u>tcatatg</u> CCTCACGGACCTCCTGAATAAA -3'<br>5' - <u>taagctt</u> CCAGACTGGTCACTGTCTTATG -3' |
| SREBP-1c | L4RE          | 5' - <u>cggtagc</u> AGATAGCCCACTTGGGTGTG -3'<br>5' - <u>tctcgag</u> CTGGAGTGCAGTGACACGAT -3'     |
| SULT2A1  | L4RE          | 5' - <u>tggtacc</u> AGTACAGGCCCGTCATTTTG -3'<br>5' - <u>cgaattc</u> AGTGATTCTCCTGCCTCAGC -3'     |
| TNFRSF4  | L4RE/Promoter | 5' - <u>ctaggtacc</u> AGTCTCGCCCTGTCGCCCA -3'<br>5' - <u>ccagagctc</u> CTCGCTGTCGCCAGAGTC -3'    |
| TNFRSF18 | L4RE/Promoter | 5' - <u>cttggtagc</u> CCCGAGTAGCTGGGATTACA -3'<br>5' - <u>ttaagctt</u> GTGTGAGGAGGGGGTGTAGA -3'  |

**Table 3. Primer sequences used in amplification of candidate target gene.** Bases in upper case represent the genomic target sequence, while underlined lower case indicates restriction enzyme sites and extra bases at the 5' end are in simple lower case.

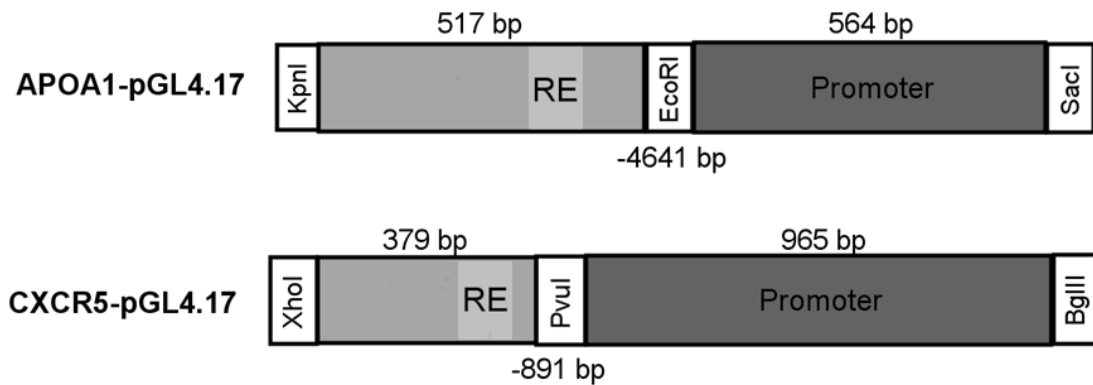


**Figure 2. Construction of luciferase plasmid inserts for APOA1 and CXCR5.** Plasmids were constructed in two separate amplicons, one containing the promoter region and one containing the RE (position indicated in light grey). Inserts were cloned into the multiple cloning site of pGL4.17 at the designated restriction sites.

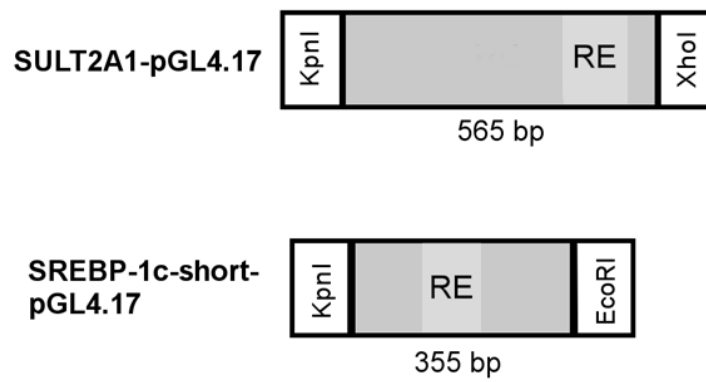


**Figure 3. Construction of luciferase plasmid inserts for SULT2A1 and SREBP-1c (short).** Plasmids were constructed from single amplicons containing only the RE (position denoted in light grey). Existing sequence was removed by restriction digest at the indicated sites, and replaced with new inserts.

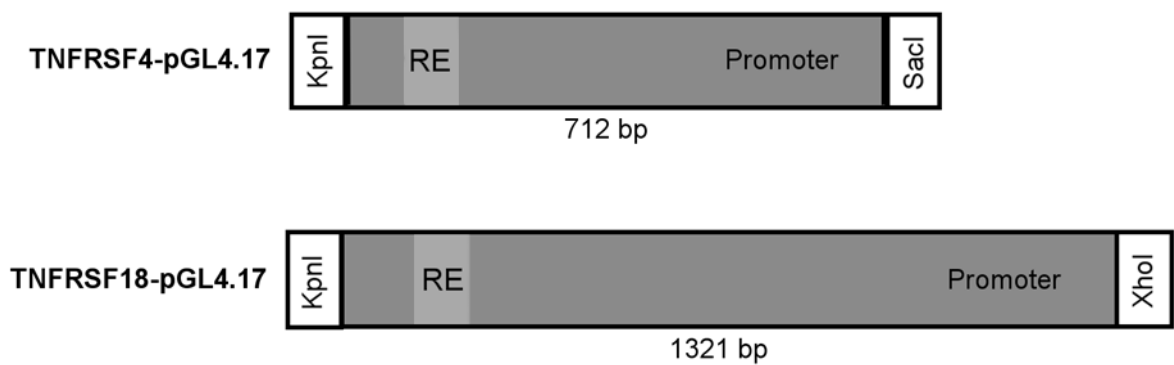


**Figure 4. Construction of luciferase plasmid inserts for TNFRSF4 and TNFRSF18.** Plasmids were constructed from single amplicons containing both the 16-nucleotide L4RE sequence (indicated in light grey) and the gene promoter, and inserted into the multiple cloning site of the pGL4.17 vector at the designated restriction sites.

## Transactivation assays

COS-7 cells were seeded in 24-well cell culture dishes and grown in Dulbecco's Modified Eagle Media (DMEM) supplemented with 10% fetal bovine serum for 8 hours at 37°C and 5% CO<sub>2</sub>. Media was then replaced with low serum DMEM and cells were transfected with 400 ng luciferase plasmid (APOA1, CXCR5, SULT2A1, SREBP1cShort, SREBP1cKnown, TNFRSF4, or TNFRSF18), 400 ng protein overexpression plasmid (PPAR $\alpha$ , LXR $\alpha$ , RXR $\alpha$ , PPAR $\alpha$  and RXR $\alpha$ , LXR $\alpha$  and RXR $\alpha$ , PPAR $\alpha$  and LXR $\alpha$ , or empty vector, pSG5), and 40 ng of pRL-CMV (Renilla luciferase driven by a CMV promoter, used as an internal control for transfection efficiency) using Lipofectamine 2000™ reagent (Invitrogen, Carlsbad, CA) and grown overnight. Transfection media was replaced with serum-free DMEM and allowed to grow another 20 hours before harvesting in lysis buffer (Promega, Madison, WI). Lysates were transferred to a 96-well microtiter plate and assayed for Firefly luciferase activity using the dual-luciferase reporter assay kit (Promega). Luminescence was measured using a BioTek Synergy plate reader (BioTek, Winooski, VT). Resulting data were normalized for transfection efficiency and the empty pSG5 vector samples for each gene were arbitrarily set to 1. Overexpression of PPAR $\alpha$ , LXR $\alpha$ , and RXR $\alpha$  proteins in cell lysates was confirmed by Western blotting.

## RESULTS

### **PPAR $\alpha$ /LXR $\alpha$ binds candidate REs *in vitro***

Electrophoretic mobility shift assays were carried out using purified full-length human proteins and an LXRE from the ABCG1 gene, as well as candidate PPAR/LXR response element oligonucleotides following a DR1, DR2, DR3, or DR4 motif. When resolved on a native gel and stained with SYBR green fluorescent dye, bands corresponding to free oligonucleotide appear at the bottom of the gel, while bands that correspond to oligonucleotide in complex with protein are retarded in migration. Since PPAR $\alpha$ /LXR $\alpha$  interaction with DNA has not been evaluated using fluorescently stained gel shifts previously, five different binding media were tested for determining optimal pH and salt concentration for PPAR $\alpha$ /LXR $\alpha$  binding to DNA (Table 2); Buffer 5 composition allowed bands which corresponded to the position of the protein bands indicated by SYPRO Ruby stain (Fig. 5C), and was thus used for subsequent experiments. Buffer 1, 2, and 4 did not result in a mobility shift (Fig.5A-B), and Buffer 3 only resulted in nonspecific shifts further in the gel (Fig. 5B). While faint shifted bands were observed in each lane, those corresponding to DR4 sequences were 2 to 3 fold more intense (Fig. 6), as quantitated by densitometry. When binding media contained only an individual protein, no binding to DNA was observed by PPAR $\alpha$  alone, consistent with that full-length PPAR $\alpha$  requires an interacting partner to bind DNA, while LXR $\alpha$  unexpectedly bound the DR4 oligonucleotides without a potential heterodimer partner present. Addition of an antibody against either protein further retarded band migration,

indicating that both proteins were present in the shifted complex. However, with addition of the PPAR $\alpha$  antibody, a portion of material failed to be supershifted, suggesting the presence of a second complex consisting only of LXR $\alpha$  bound to DNA (Fig. 7).



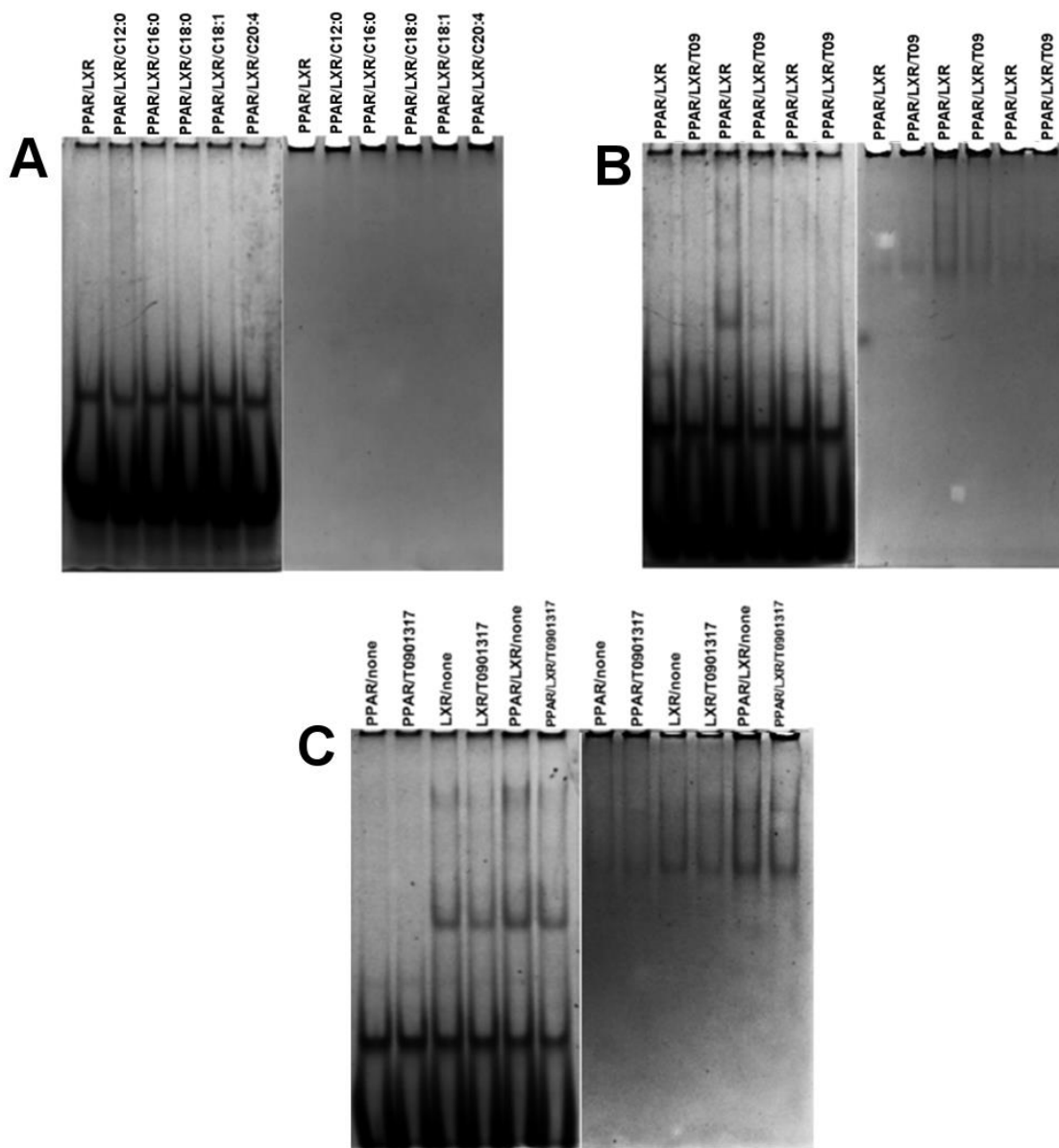


**Figure 5. Preliminary EMSAs of PPAR $\alpha$ /LXR $\alpha$  with ABCG1 LXRE for buffer optimization.** SYBR Green (left) and SYPRO Ruby (right) stains of EMSA experiments with Buffer 1 (A), Buffer 2 (B, lanes 1 and 2), Buffer 3 (B, lanes 3 and 4), Buffer 4 (B, lanes 5 and 6), and Buffer 5 (C). Buffer 5 alone demonstrated binding.

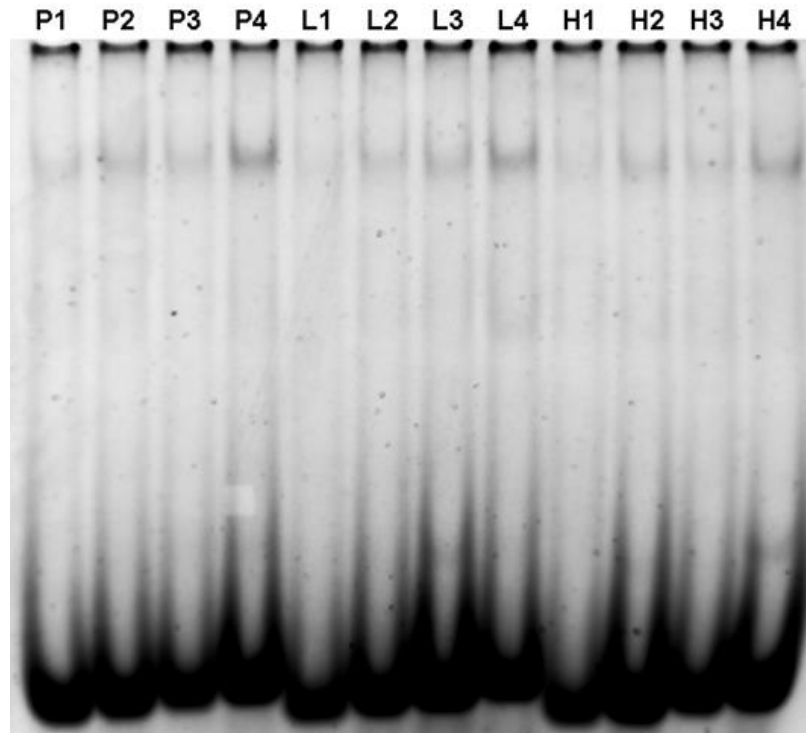


**Figure 6. EMSA of PPAR $\alpha$ /LXR $\alpha$  with candidate response elements showing preference for DR4 element.** 200 ng each of PPAR $\alpha$  and LXR $\alpha$  were incubated with 40 ng of candidate RE oligonucleotides and resolved on 6% non-denaturing polyacrylamide gels. Bands representing bound PPRE-like (P), LXRE-like (L), or hybrid (H) sequences separated by 4 nucleotides exhibited the highest band intensity.

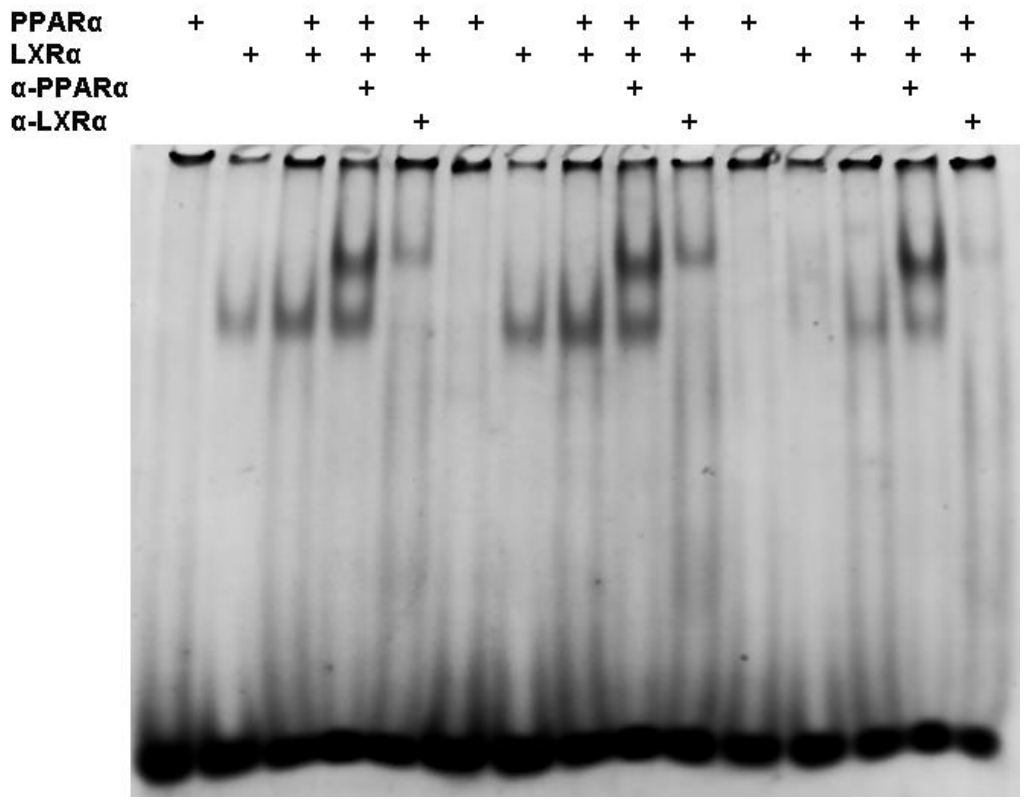


**Figure 7. Supershift assay demonstrating presence of both PPAR $\alpha$  and LXR $\alpha$  in complex with DNA.** The protein-DNA complex is shifted further upward in the gel with the addition of an antibody against PPAR $\alpha$  or LXR $\alpha$ . However, the entire complex is not shifted with the PPAR $\alpha$  antibody, but is entirely shifted with the LXR $\alpha$  antibody, suggesting the presence of a second complex consisting of only LXR $\alpha$  bound to DNA.

### **PPAR $\alpha$ /LXR $\alpha$ and LXR $\alpha$ alone bind candidate REs with nanomolar affinity**

Since EMSAs only provide a qualitative representation of protein-DNA interactions *in vitro*, it was necessary to examine the ability of PPAR $\alpha$ /LXR $\alpha$  to bind DNA in a manner that would yield quantitative information at concentrations that are physiologically relevant in the cell. To that end, intrinsic protein fluorescence quenching experiments were conducted, wherein changes in fluorescence emission by aromatic amino acid residues in the protein as a function of DNA oligonucleotide concentration were measured and reflect conformational changes in the protein induced by DNA binding. The change in fluorescence emission was plotted as a function of the total concentration of DNA titrated allows for an estimation of binding affinity.

PPAR $\alpha$  does not bind DNA without an interacting protein partner, which is consistent with the absence of shifted bands observed in EMSA experiments (Fig. 7). To confirm those results, 100 nM PPAR $\alpha$  was titrated against increasing concentrations of the three candidate REs, as well as the known ACOX PPRE and SREBP LXRE. Intuitively, the only candidate RE to exhibit binding saturation was the P4RE, whereas the L4RE titration only resulted in a relatively weak change in fluorescence intensity without exhibiting saturation (Fig. 8). While the P4RE and H4RE titrations did result in a dramatic decrease in fluorescence intensity with a low apparent  $K_d$  value (see Table 4), the resulting plot of fluorescence intensity against DNA concentration suggests that the sample failed to reach saturation within the range of DNA concentrations tested. This indicates that any interaction occurring was weak or non-specific at best. PPAR $\alpha$  also failed to reach saturation when titrated with ACOX PPRE or SREBP LXRE (Fig. 9),

further establishing that PPAR $\alpha$  binds DNA only in a weak or non-specific manner in the absence of a heterodimeric partner.

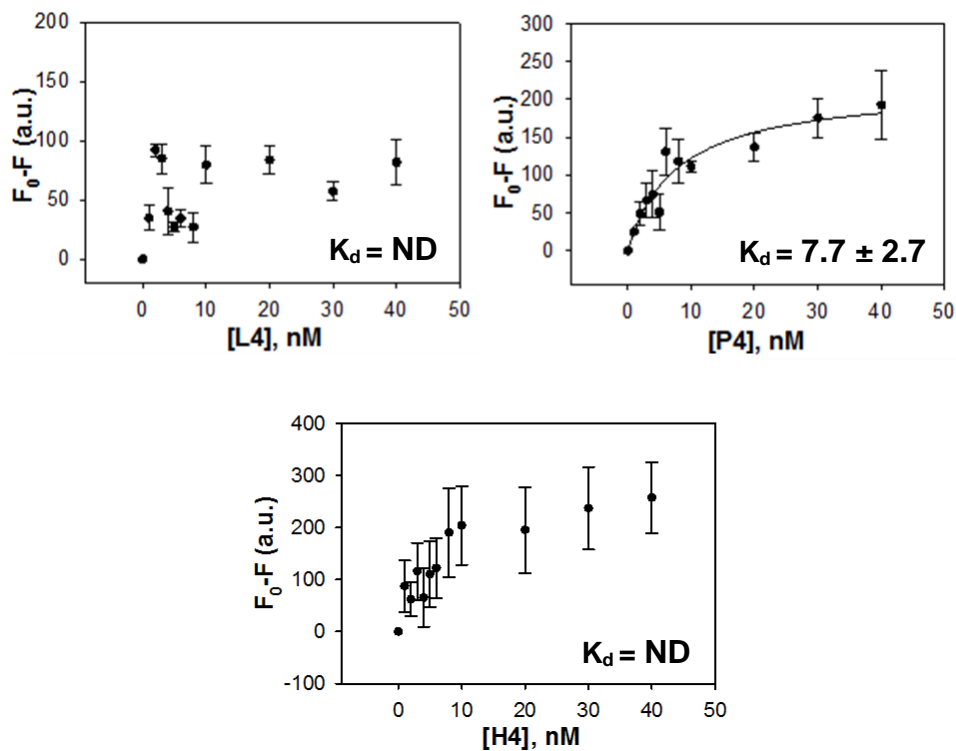


**Figure 8. Intrinsic fluorescence quenching of PPAR $\alpha$  upon titration with candidate REs.** 100 nM PPAR $\alpha$  was titrated against increasing concentrations of oligonucleotide, and the change in fluorescence intensity was plotted against DNA concentration to obtain apparent  $K_d$ . Data are represented as mean  $\pm$  S.E.,  $n \geq 3$ .

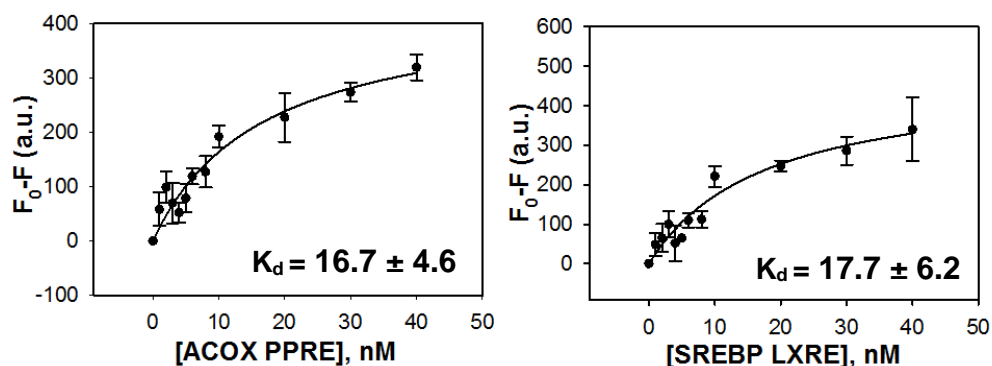


**Figure 9. Intrinsic fluorescence quenching of PPAR $\alpha$  upon titration with known REs.** 100 nM PPAR $\alpha$  was titrated against increasing concentrations of oligonucleotide, and the change in fluorescence intensity was plotted against DNA concentration to obtain apparent  $K_d$ . Data are represented as mean  $\pm$  S.E.,  $n \geq 3$ .

Alternatively, when examining 100 nM LXR $\alpha$  interaction with RE oligonucleotides, LXR $\alpha$  produced high affinity binding curves with a less intense change in fluorescence. LXR $\alpha$  bound all three candidate REs with affinities of less than 5 nM (Fig. 10), which clearly showed saturation, suggesting that LXR $\alpha$  is able to bind these REs with high affinity, and in the absence of a heterodimeric interacting partner. Further, LXR $\alpha$  bound the ACOX PPRE and the SREBP LXRE (Fig. 11), although the curve produced from the PPRE data was not as pronounced, and thus was bound with lower affinity.

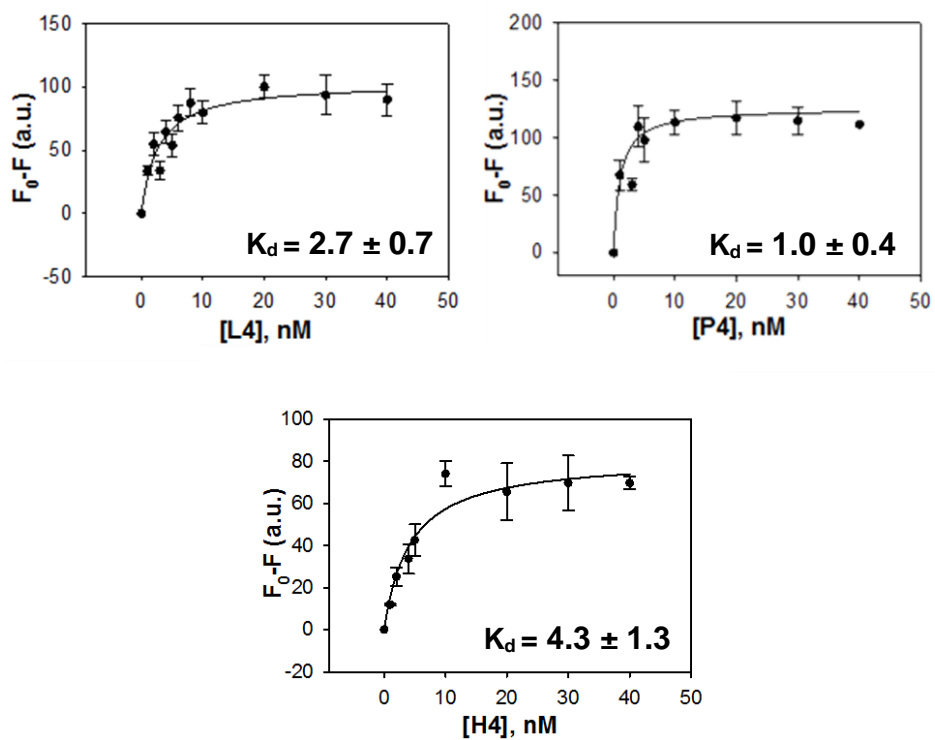


**Figure 10. Intrinsic fluorescence quenching of LXR $\alpha$  upon titration with candidate REs.** 100 nM LXR $\alpha$  was titrated against increasing concentrations of oligonucleotide, and the change in fluorescence intensity was plotted against DNA concentration to obtain apparent  $K_d$ . Data are represented as mean  $\pm$  S.E.,  $n \geq 3$ .

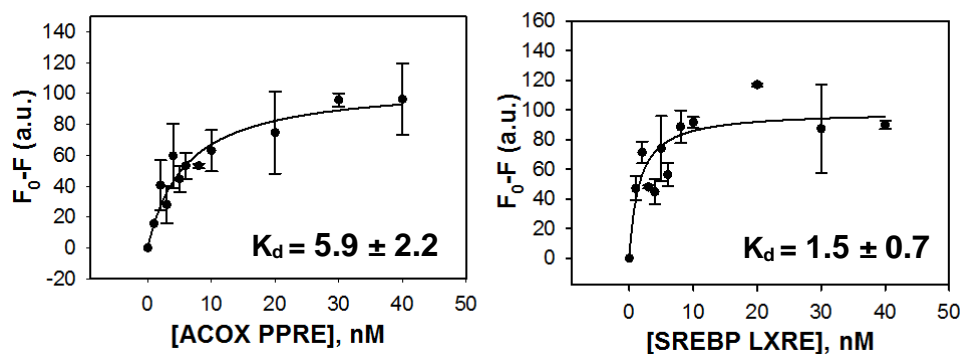


**Figure 11. Intrinsic fluorescence quenching of LXR $\alpha$  upon titration with known REs.** 100 nM LXR $\alpha$  was titrated against increasing concentrations of oligonucleotide, and the change in fluorescence intensity was plotted against DNA concentration to obtain apparent  $K_d$ . Data are represented as mean  $\pm$  S.E.,  $n \geq 3$ .

The PPAR $\alpha$ /LXR $\alpha$  mixture bound the P4RE, L4RE, and H4RE oligonucleotides with  $K_d$  values in the low nanomolar range and indicative of high affinity binding (Fig. 12), which confirmed the results of the EMSA experiments. Of the three, the L4RE and H4RE bound with the highest affinity, around 2 nM, with the P4RE only slightly lower affinity at around 5 nM. Interestingly, binding to either the ACOX PPRE or the SREBP-1c LXRE was not detected (Fig. 13). Furthermore, transforming the binding data for the L4RE and the H4RE into a Hill plot yields a slope of  $<1$ , indicating at least two negatively cooperative binding sites are present (Fig. 14). Taken together with the overall shape of the curves, which seem to reach saturation early but climb again around the highest concentrations, this suggests a transition from high affinity binding to low affinity binding, presumably represented respectively by LXR $\alpha$  and PPAR $\alpha$ .



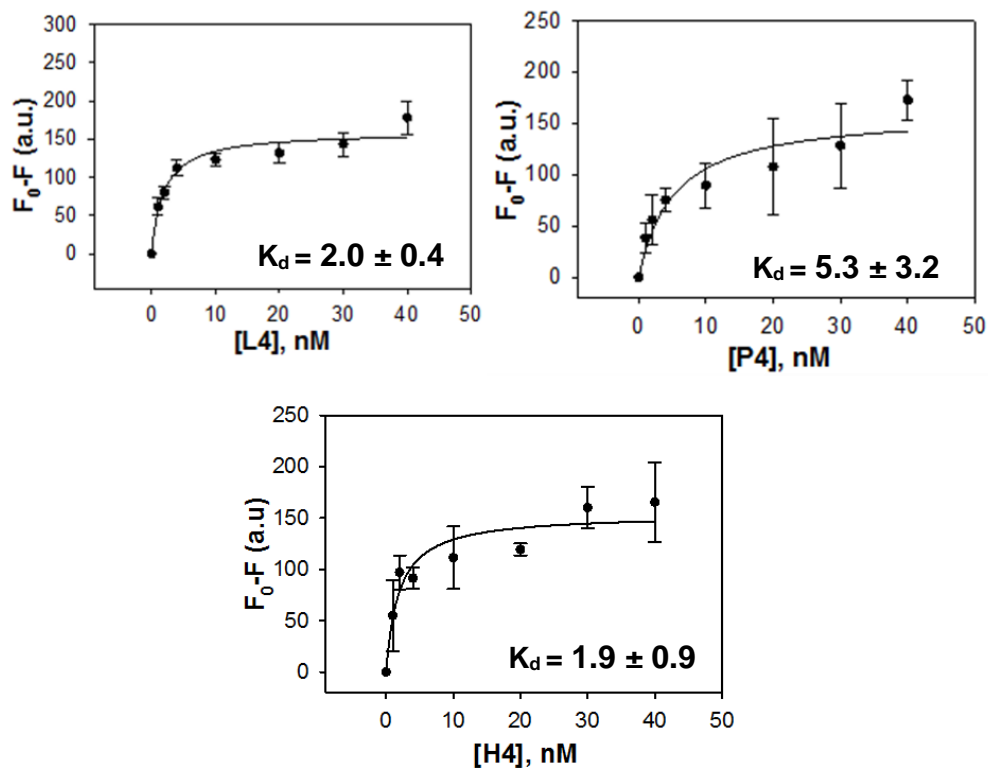


**Figure 12. Intrinsic fluorescence quenching of PPAR $\alpha$ /LXR $\alpha$  upon titration with candidate REs.** 50 nM each PPAR $\alpha$  and LXR $\alpha$  (1:1, total 100 nM protein) was titrated against increasing concentrations of oligonucleotide, and the change in fluorescence intensity was plotted against DNA concentration to obtain apparent  $K_d$ . Data are represented as mean  $\pm$  S.E.,  $n \geq 3$ .

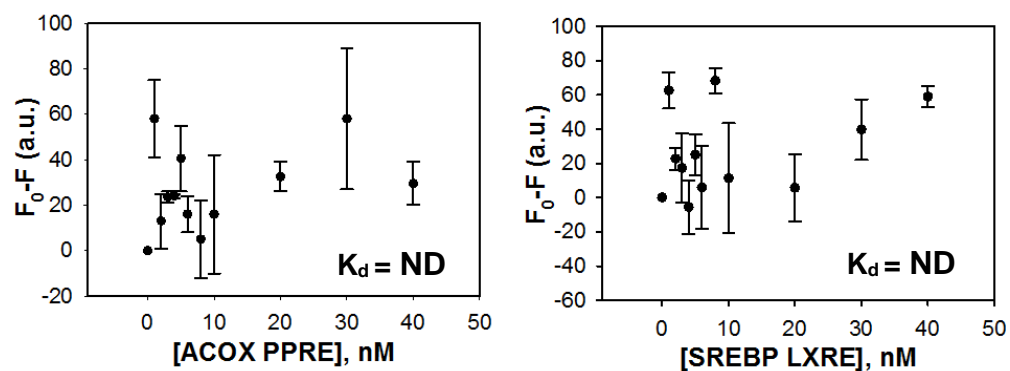


**Figure 13. Intrinsic fluorescence quenching of PPAR $\alpha$ /LXR $\alpha$  upon titration with known REs.** 50 nM each PPAR $\alpha$  and LXR $\alpha$  (1:1, total 100 nM protein) was titrated against increasing concentrations of oligonucleotide, and the change in fluorescence intensity was plotted against DNA concentration to obtain apparent  $K_d$ . Data are represented as mean  $\pm$  S.E.,  $n \geq 3$ .

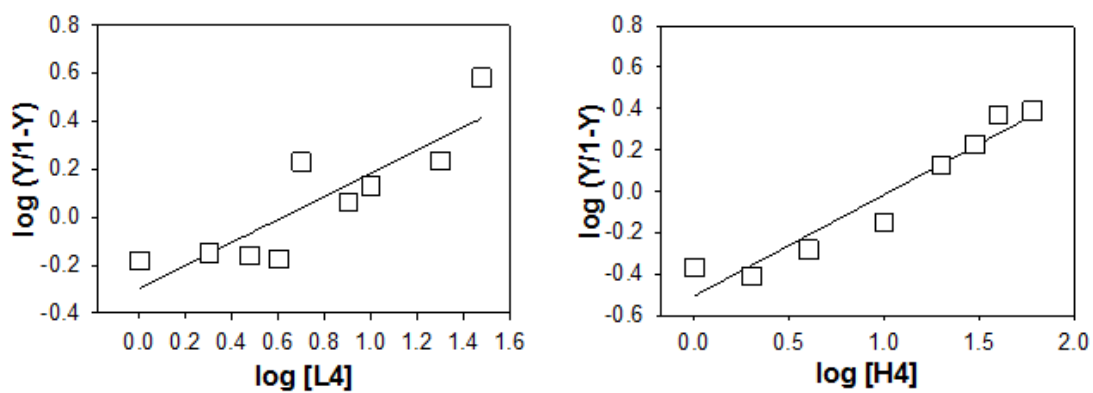


**Figure 14. Plotting PPAR $\alpha$ /LXR $\alpha$  binding data on Hill coordinates suggests multiple binding sites.** Plots were generated by calculating partial saturation (Y) from the change in fluorescence intensity, and plotting the log of (Y/1-Y) against the log of the oligonucleotide concentration. The slopes of the lines were 0.4795 for the L4RE, and 0.4901 for the H4RE, indicating negative cooperativity and, thus, multiple binding sites.

|                   | <b>PPAR</b>    | <b>LXR</b>    | <b>PPAR/LXR</b> |
|-------------------|----------------|---------------|-----------------|
| <b>L4</b>         | ND             | $2.7 \pm 0.7$ | $2.0 \pm 0.4$   |
| <b>P4</b>         | $7.7 \pm 2.7$  | $1.0 \pm 0.4$ | $5.3 \pm 3.2$   |
| <b>H4</b>         | ND             | $4.3 \pm 1.3$ | $1.9 \pm 0.9$   |
| <b>ACOX PPRE</b>  | $16.7 \pm 4.6$ | $5.9 \pm 2.2$ | ND              |
| <b>SREBP LXRE</b> | $17.7 \pm 6.2$ | $1.5 \pm 0.7$ | ND              |

**Table 4. Binding affinities of PPAR $\alpha$ , LXR $\alpha$ , and PPAR $\alpha$ /LXR $\alpha$  for known and candidate REs.** Apparent  $K_d$  values (nM) were obtained for all experiments,  $n \geq 3$ . Lower values indicate higher affinity binding.

## Candidate REs occur naturally in the human genome

Chromatin immunoprecipitation (ChIP) is an effective way to gauge protein-DNA interactions in a cell-based environment, and is a powerful tool for determining sequence specificity when combined with high-throughput next generation sequencing (ChIP-seq). Previous ChIP-seq studies were used to address whether the L4RE, P4RE, or H4RE sequences were bound by PPAR $\alpha$  and LXR $\alpha$ . Sequential ChIP-seq, which would show DNA sequences bound by PPAR $\alpha$  and LXR $\alpha$  simultaneously, is very difficult to perform due to the small amount of bound DNA recovered from such experiments. Information from ChIP-seq data was limited to overlap between ChIP-seq experiments performed with antibodies against PPAR $\alpha$  and LXR $\alpha$  individually.

2655 LXR $\alpha$  sites across the genome were obtained from [42], which were already mapped to Hg19. 1920 sites were present in the overlap from Hg19-mapped mouse data from [31], although they were not identical to those from the LXR $\alpha$  only data. The P4RE sequence yielded a single hit on chromosome 12, while the H4RE was not present at all in a search of Hg19. The L4RE, however, occurred 87,486 times, with e values ranging from 0.027 to 0.004, indicating that hits did not occur due to random chance (Fig.15, Bottom). The data sets for the overlap, LXR $\alpha$ -only, and L4RE sites do not overlap, although there are sites located in close proximity (Fig.15, Middle).

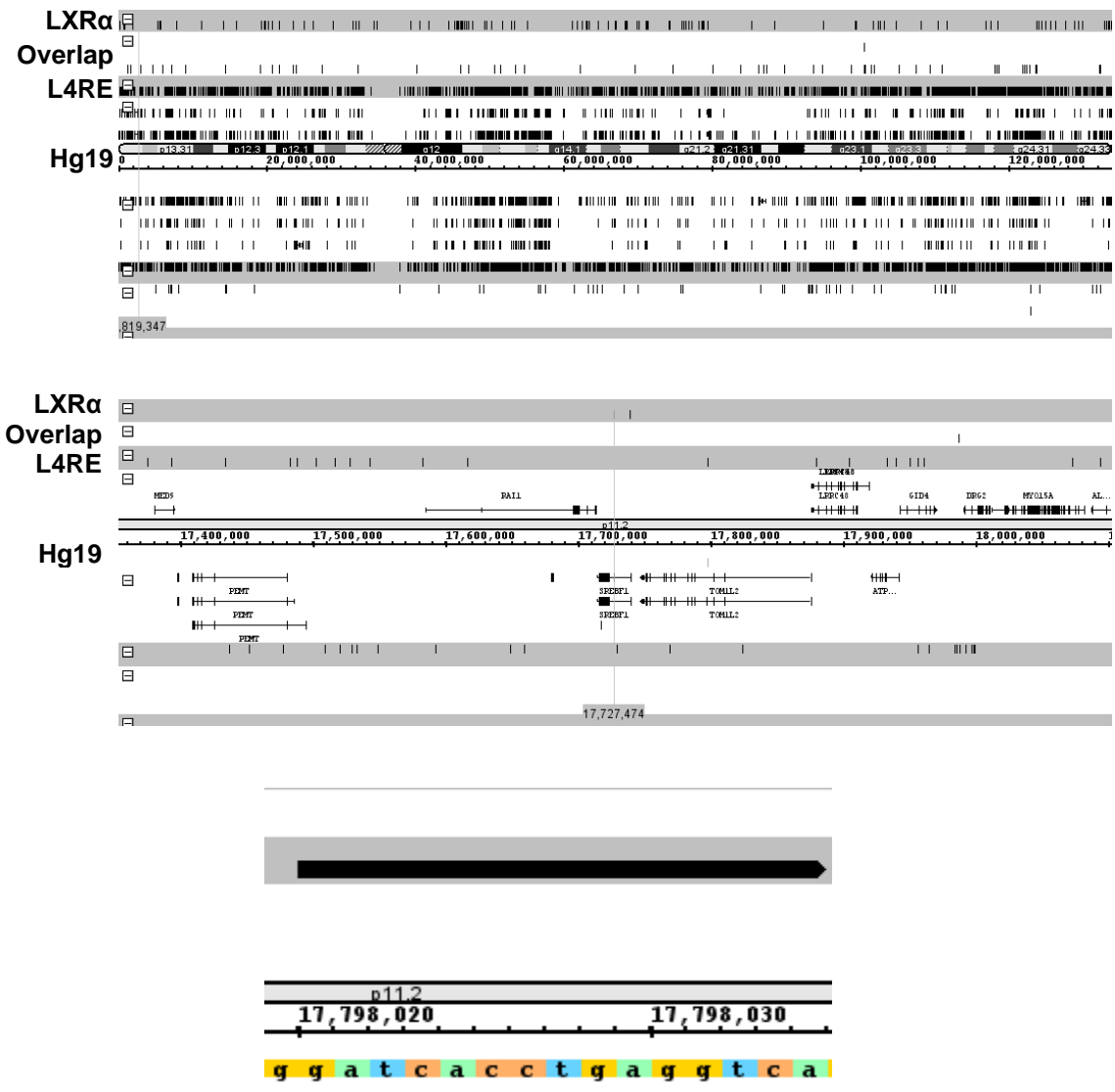


**Figure 15. Genomic locations of the L4RE candidate response element relative to known PPAR $\alpha$  and LXR $\alpha$  binding sites. Top:** Integrated Genome Browser view of chromosome 12 of the Hg19 human genome assembly, with tracks generated from ChIP-seq data for LXR $\alpha$  alone, an overlap of ChIP-seq data for PPAR $\alpha$  and LXR $\alpha$ , and the L4RE candidate response element. **Middle:** Expanded view of chromosome 17, with the position of the *SREBF1* gene indicated with a vertical grey line, demonstrating a lack of overlap between the three sets. **Bottom:** Close view of a representative L4RE site demonstrating an exact match to the sequence used *in vitro*.

## **PPAR $\alpha$ /LXR $\alpha$ and LXR $\alpha$ alone transactivate endogenous promoters**

Once the ability of PPAR $\alpha$ /LXR $\alpha$  to bind the candidate RE sequences was established *in vitro* via EMSAs and binding experiments, the possible functional consequences of such binding in a cell-based environment were determined. To accomplish this, a BLAST search of the human genome for the candidate REs yielded many instances of an exact match to the L4RE sequence. The search was narrowed to only include sequences within 5 kilobases of a known or identified promoter element, of which 6 were chosen for further study. *APOA1*, *SULT2A1*, and *SREBF1* are all known to be regulated by either PPAR $\alpha$  or LXR $\alpha$ , or by both. Additionally, occurrences near *CXCR5*, *TNFRSF4*, and *TNFRSF18* were also chosen in order to examine the possibility that a distinct subset of genes are regulated by the PPAR $\alpha$ /LXR $\alpha$  heterodimer rather than being regulated by the PPAR $\alpha$  or LXR $\alpha$  heterodimers, and also that genes expressed in different tissues (B cells and T cells, in this case) respond to regulatory stimulation from PPAR $\alpha$  and/or LXR $\alpha$  differently. Portions of genomic DNA containing the target L4RE sequence and the endogenous gene promoters were cloned into the pGL4.17 promoterless luciferase reporter plasmid (Fig. 2-4), and transactivation assays were performed to assess the ability of PPAR $\alpha$  and LXR $\alpha$ , transiently overexpressed via pSG5 expression constructs, to alter RE activity in COS-7 cells. Overexpression of transfected proteins was determined immediately following each replicate by Western blotting, which showed a marked increase in protein levels in cells transfected with one or both overexpression plasmids (Fig. 16). However, the expression of both proteins does not increase so

strongly in cells which were co-transfected with both PPAR $\alpha$  and LXR $\alpha$  expression plasmids.

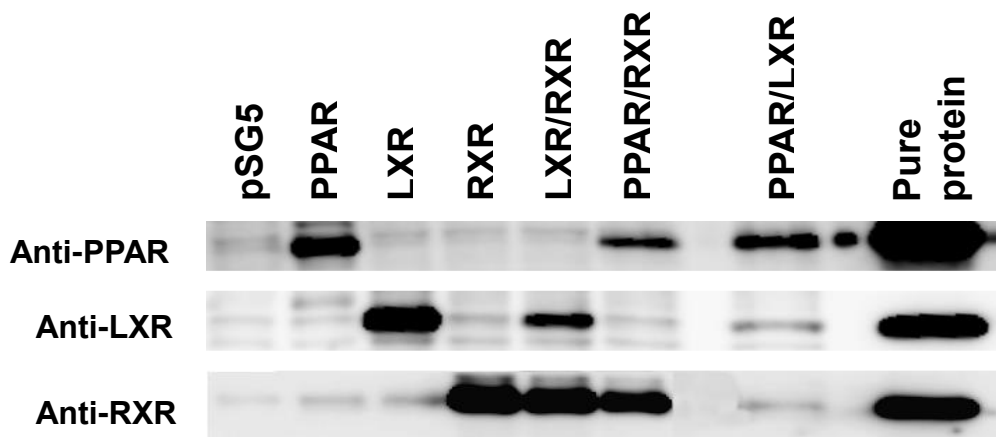


**Figure 16. Western blot showing overexpression of transiently transfected PPAR $\alpha$ , LXR $\alpha$ , and RXR $\alpha$ .** Lysates from COS-7 cells transfected with the indicated plasmids were run on 10% SDS-PAGE gels, transferred to nitrocellulose membranes and probed with antibodies against PPAR $\alpha$ , LXR $\alpha$ , and RXR $\alpha$ .



The APOA1-pGL4.17 plasmid was constructed from two separate amplicons, one 564 bp fragment containing the promoter machinery, and another 517 bp fragment which contained the L4RE sequence, omitting 4641 bp between them. Transactivation of this reporter remained at basal levels in cells transfected with the pSG5-PPAR $\alpha$  plasmid alone, nearly identical to those cells transfected only with empty pSG5 vector. In contrast, cells transfected with pSG5-LXR $\alpha$  demonstrated significantly increased L4RE transactivation, approximately 3- to 4-fold higher than vector alone (Fig. 17). Although some RXR $\alpha$  is present in COS-7 cells, transactivation is not significantly increased from this level when RXR $\alpha$  is co-overexpressed, suggesting that this finding is not dependent on levels of that protein and is, in fact, a result of LXR $\alpha$  activity, potentially as a homodimer. Significantly increased transactivation was also observed when PPAR $\alpha$  and LXR $\alpha$  were co-overexpressed, although the increase was not as strong as that from cells transfected with LXR $\alpha$  alone and appeared to indicate that the presence of PPAR $\alpha$  inhibits LXR $\alpha$  activity. Taken together, these results suggest that not only could PPAR $\alpha$ /LXR $\alpha$  heterodimers transactivate this L4RE and alter expression of the *APOA1* gene, LXR $\alpha$  may also do so as a homodimer.

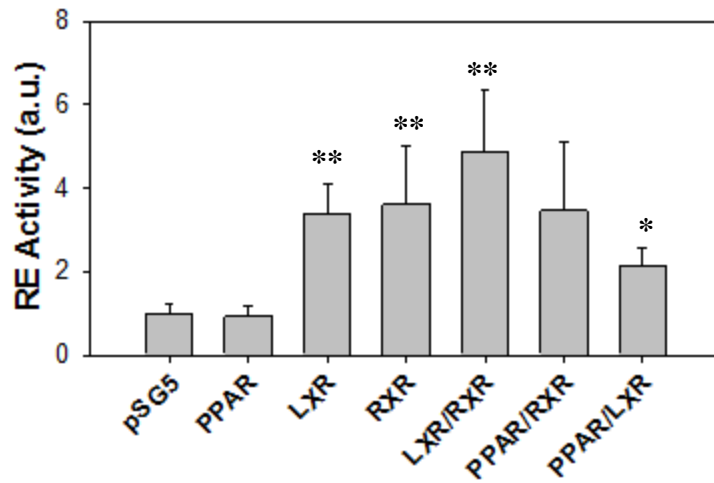


**Figure 17. Transactivation of APOA1.** Transiently overexpressed proteins are noted on the x-axis, and the y-axis represents normalized relative activity of the indicated RE. Asterisks denote statistical significance from pSG5 vector-treated cells as determined by student's t-test, with \* =  $p > 0.05$ , \*\* =  $p > 0.005$ , and \*\*\* =  $p > 0.001$ . Data are represented as mean  $\pm$  S.E.,  $n \geq 4$ .

The construction of the CXCR5-pGL4.17 plasmid was similar to that of APOA1-pGL4.17, with a 965 bp fragment containing the TATA-less promoter [44] and a 379 bp fragment with the response element and only 891 bp omitted between them. This plasmid, however, was not as responsive to transactivation by exogenous PPAR $\alpha$  and LXR $\alpha$  (Fig. 18). Only cells transfected with pSG5-LXR $\alpha$  alone demonstrated significantly increased luciferase expression, and only reaching about 2-fold higher expression levels than the vector control. Cells overexpressing PPAR $\alpha$  alone showed a slight decrease in RE activity, while those transfected with both PPAR $\alpha$  and LXR $\alpha$  increased transactivation only minimally. These data indicate that CXCR5 is not likely a target of these two proteins, but may be affected by LXR $\alpha$  alone.

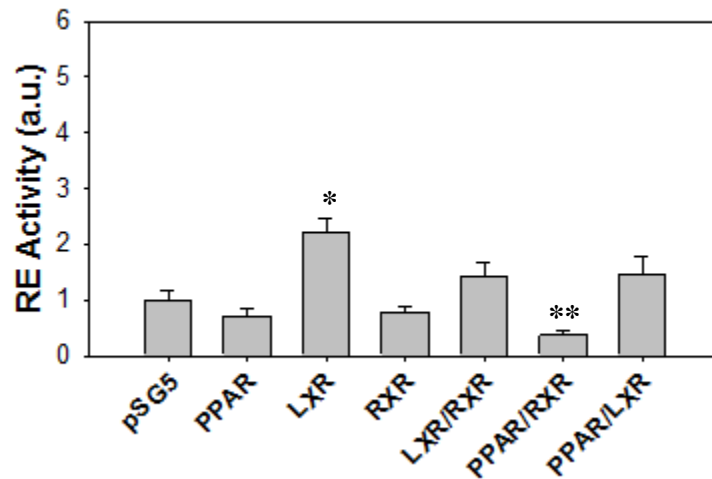


**Figure 18. Transactivation of CXCR5.** Transiently overexpressed proteins are noted on the x-axis, and the y-axis represents normalized relative activity of the indicated RE. Asterisks denote statistical significance from pSG5 vector-treated cells as determined by student's t-test, with \* =  $p > 0.05$ , \*\* =  $p > 0.005$ , and \*\*\* =  $p > 0.001$ . Data are represented as mean  $\pm$  S.E.,  $n \geq 4$ .

The *SULT2A1* promoter was previously cloned into pGL4.17 by Mrs. Jeannette Manger, and a 565 bp fragment containing the L4RE was inserted into the existing plasmid in order to complete SULT2A1-pGL4.17. Transfection with pSG5-PPAR $\alpha$  affected a minor decrease in RE activity, although not enough to be statistically significant. In a similar trend to that seen with APOA1 and CXCR5, RE activity increased significantly in cells transfected only with pSG5-LXR $\alpha$ , and co-transfection of both PPAR $\alpha$  and LXR $\alpha$  overexpression plasmids also resulted in an increase in RE activity. However, like the change seen with PPAR $\alpha$  alone, this difference was not determined to be statistically significant. Once again, it seemed that LXR $\alpha$  was able to affect transactivation of this promoter through the L4RE response element in the absence of PPAR $\alpha$  as a heterodimer partner (Fig. 19).

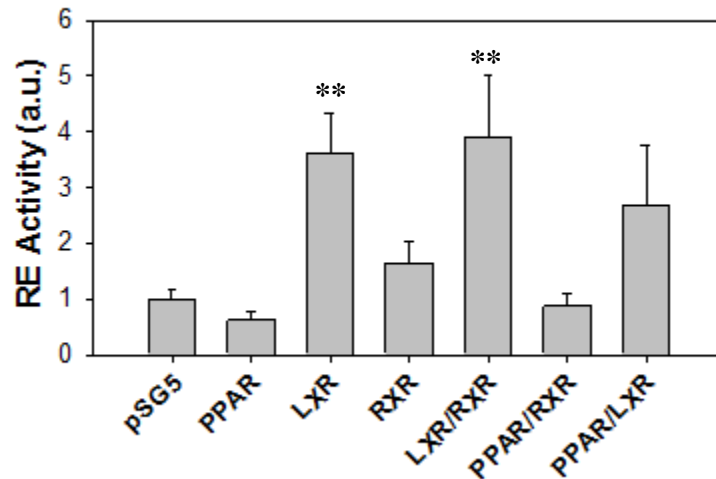


**Figure 19. Transactivation of SULT2A1.** Transiently overexpressed proteins are noted on the x-axis, and the y-axis represents normalized relative activity of the indicated RE. Asterisks denote statistical significance from pSG5 vector-treated cells as determined by student's t-test, with \* =  $p > 0.05$ , \*\* =  $p > 0.005$ , and \*\*\* =  $p > 0.001$ . Data are represented as mean  $\pm$  S.E.,  $n \geq 4$ .

*SREBF1* is a well-characterized target of both PPAR $\alpha$  and LXR $\alpha$ , and its promoter region contains two known LXREs, as well as a PPRE through which PPAR $\alpha$  may repress LXR $\alpha$ -mediated upregulation of the gene. The L4RE sequence was located approximately 2 kb upstream of the promoter, and thus, two luciferase plasmids were tested for SREBP-1c: a construct previously cloned in the lab termed SREBP-1c-known-pGL4.17, which contains the endogenous promoter with the known PPAR $\alpha$  and LXR $\alpha$  response elements, as well as a plasmid containing a 355 bp fragment containing the L4RE located near the gene inserted upstream of the promoter, with the known REs removed, henceforth referred to as SREBP-1c-short-pGL4.17. When cells only overexpressing PPAR $\alpha$  were examined, there was again no significant change from basal transactivation levels observed, with either SREBP-1c plasmid. Likewise, there was no significant change in transactivation when both proteins were co-overexpressed, indicating that the PPAR $\alpha$ /LXR $\alpha$  heterodimer is not capable of transactivating the L4RE (Fig. 20), or the known PPRE and LXREs (Fig. 21), with the *SREBF1* promoter. However, cells transfected with LXR $\alpha$  alone again demonstrated significantly increased transactivation of the known REs, but not of the L4RE. These data are intriguing due to the fact that SREBP-1c, as a major regulator of fatty acid synthesis in the cell, is of concern when targeting LXR $\alpha$  for therapeutic purposes, and it is interesting to note that while PPAR $\alpha$ /LXR $\alpha$  appears to be able to transactivate *APOA1*, an effect that would be beneficial for such an application, it does not transactivate *SREBF1* and may thus provide an avenue through which to target LXR $\alpha$  while bypassing the negative side effects from attempts which target the LXR $\alpha$ /RXR $\alpha$  heterodimer.

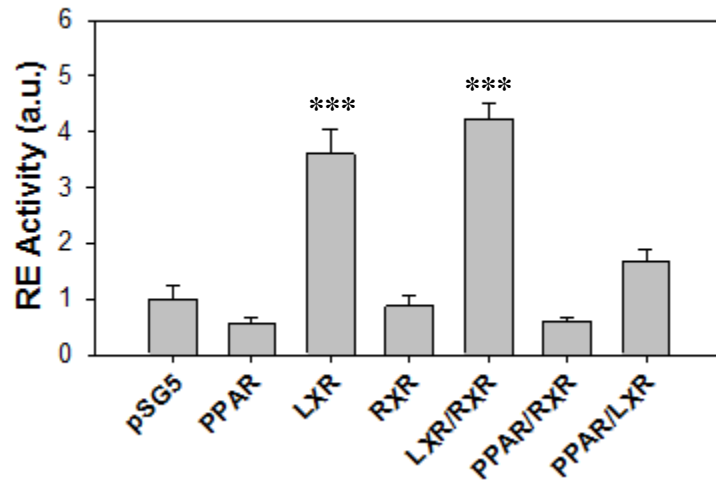


**Figure 20. Transactivation of SREBP-1c (known PPRE and LXREs).** Transiently overexpressed proteins are noted on the x-axis, and the y-axis represents normalized relative activity of the indicated RE. Asterisks denote statistical significance from pSG5 vector-treated cells as determined by student's t-test, with \* =  $p > 0.05$ , \*\* =  $p > 0.005$ , and \*\*\* =  $p > 0.001$ . Data are represented as mean  $\pm$  S.E.,  $n \geq 4$ .

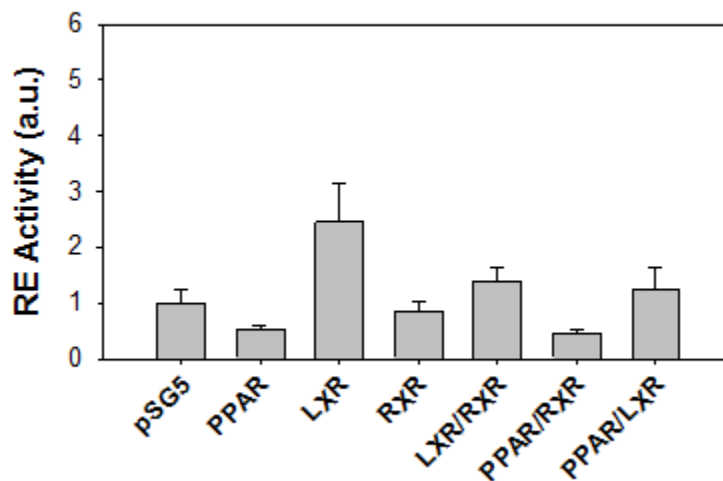


**Figure 21. Transactivation of SREBP-1c (L4RE only).** Transiently overexpressed proteins are noted on the x-axis, and the y-axis represents normalized relative activity of the indicated RE. Asterisks denote statistical significance from pSG5 vector-treated cells as determined by student's t-test, with \* =  $p > 0.05$ , \*\* =  $p > 0.005$ , and \*\*\* =  $p > 0.001$ . Data are represented as mean  $\pm$  S.E.,  $n \geq 4$ .

*TNFRSF4* and *TNFRSF18* are members of the tumor necrosis factor receptor superfamily, and are alternatively known as OX40 and GITR, respectively. Both genes are located in close proximity to an incidence of the L4RE, and thus it was possible to amplify the promoter region and the L4RE within the same fragment to construct *TNFRSF4*-pGL4.17 and *TNFRSF18*-pGL4.17. PPAR $\alpha$  overexpression resulted in a decrease in transactivation of both of these plasmids, *TNFRSF18* (Fig. 23) more so than *TNFRSF4* (Fig. 22), but neither was statistically significant. PPAR $\alpha$ /LXR $\alpha$  co-overexpression also failed to raise transactivation significantly above that displayed by vector-treated cells. As previously shown, only cells overexpressing LXR $\alpha$  alone exhibited a statistically significant increase in transactivation.

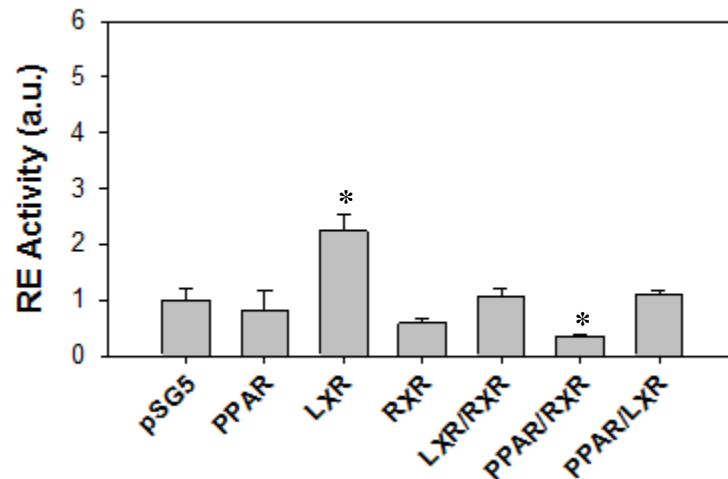


**Figure 22. Transactivation of *TNFRSF4*.** Transiently overexpressed proteins are noted on the x-axis, and the y-axis represents normalized relative activity of the indicated RE. Asterisks denote statistical significance from pSG5 vector-treated cells as determined by student's t-test, with \* =  $p > 0.05$ , \*\* =  $p > 0.005$ , and \*\*\* =  $p > 0.001$ . Data are represented as mean  $\pm$  S.E.,  $n \geq 4$ .



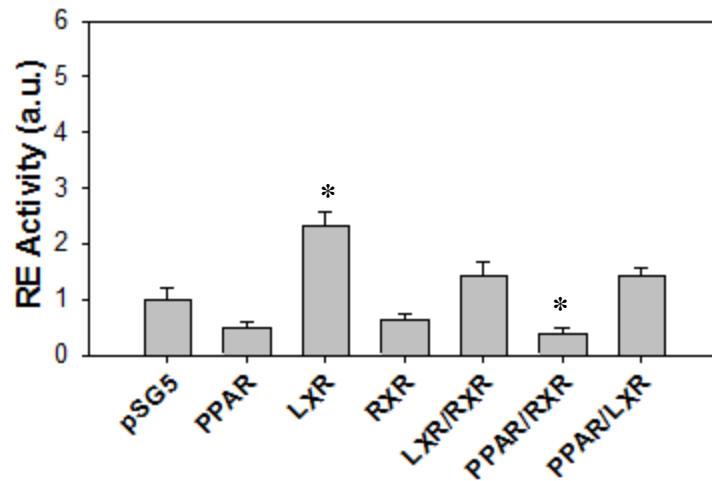


**Figure 23. Transactivation of TNFRSF18.** Transiently overexpressed proteins are noted on the x-axis, and the y-axis represents normalized relative activity of the indicated RE. Asterisks denote statistical significance from pSG5 vector-treated cells as determined by student's t-test, with \* =  $p > 0.05$ , \*\* =  $p > 0.005$ , and \*\*\* =  $p > 0.001$ . Data are represented as mean  $\pm$  S.E.,  $n \geq 4$ .

Taken together, the results of transactivation experiments suggested that, while PPAR $\alpha$ /LXR $\alpha$  may be able to affect expression of *APOA1* via the L4RE, it is unable to do so with the other genes tested. Furthermore, LXR $\alpha$  was consistently able to transactivate these REs without an overexpressed heterodimer partner.

## DISCUSSION

Energy homeostasis and metabolism are comprised of a host of interweaving processes governed by tight transcriptional regulation of the expression of relevant genes. PPAR $\alpha$  and LXR $\alpha$  both play a vital role in this regulation through control of genes involved in the oxidation and synthesis of fatty acids, as well as efflux, transport, and metabolism of cholesterol. However, energy homeostasis is, by nature, complex, as are the mechanisms by which the pathways involved are modulated, and as such the full extent of the coordination between these two proteins is not entirely understood. This study aimed to broaden the understanding of the intricacies of metabolic regulation as it related to PPAR $\alpha$  and LXR $\alpha$  by demonstrating that these two proteins, as a heterodimer, bind to DNA, specifically and with high affinity, and exact a physiological consequence.

Direct interaction between full-length, human PPAR $\alpha$  and LXR $\alpha$  was successfully demonstrated by Balanarasimha et al., as was binding of the proteins to the ACOX PPRE and the SREBP-1c LXRE via electrophoretic mobility shift assays. Miyata et al. attempted to show PPAR $\alpha$ /LXR $\alpha$  binding to DNA using idealized AGGTCA\_AGGTCA response element sequences, separated by 0 to 5 nucleotides, but were unable to do so. It is important to consider that those and other studies were conducted using murine, tagged, and/or truncated versions of one or both proteins. Specifically, those experiments were conducted using murine PPAR $\alpha$  and human LXR $\alpha$ . While valuable as a basis for future study, such experiments do not provide an accurate representation of the true DNA binding characteristics of the proteins. Incorporation of affinity tags and truncating

proteins may alter the structure of the proteins, which may cause changes in its function. Likewise, while there is significant sequence homology between mouse and human PPAR $\alpha$  and LXR $\alpha$ , the functions differ slightly by species. For example, in mice, LXR $\alpha$  is a known regulator of cholesterol-7 $\alpha$ -hydroxylase, or CYP7A1, but does not regulate the same gene in humans. Similarly, peroxisome proliferation seen in mice in response to PPAR $\alpha$  ligands has not been observed in humans, and mouse and human PPAR $\alpha$  have been shown to respond differently to binding of endogenous ligands. Thus, this study conducted EMSA and fluorescence quenching experiments using full-length, human PPAR $\alpha$  and LXR $\alpha$ . The fact that even an idealized DR4 sequence did not bind raised the possibility that DNA binding by PPAR $\alpha$ /LXR $\alpha$  heterodimers has a different DNA sequence specificity than RXR $\alpha$  heterodimers. Thus, this study designed candidate PPAR $\alpha$ /LXR $\alpha$  response elements using half-sites from consensus data for PPREs and LXREs, which were degenerate from the idealized RE sequence.

This work demonstrated, *in vitro*, that PPAR $\alpha$  and LXR $\alpha$  bind DNA as a heterodimer with a clear preference for a DR4 response element. While bands with low intensity were observed in lanes with the DR1, DR2, and DR3 elements, those in the DR4 lanes were significantly more intense. While binding reactions in which only PPAR $\alpha$  was present did not result in a shifted complex, which is consistent with previously published data, shifts were observed, intriguingly, where only LXR $\alpha$  was present. Supershift assays were performed to assess and confirm the presence of both proteins in the shifted complex. Additional retardation in the gel was observed using either an antibody against PPAR $\alpha$  or against LXR $\alpha$ , indicating that the shifted complex consisted of both PPAR $\alpha$  and LXR $\alpha$  bound to DNA. While bands indicating binding to the H4RE

were slightly less intense than the P4RE or the L4RE, PPAR $\alpha$ /LXR $\alpha$  heterodimers did not demonstrate specificity for any of these particular sets of half-sites. However, binding to all three candidate REs was more intense than binding to the ACOX PPRE or the SREBP-1c LXRE, supported by additional fluorescence quenching experiments. This failure to bind more degenerate REs suggests that PPAR $\alpha$ /LXR $\alpha$  heterodimers may have greater sequence specificity with respect to its target sequences than PPAR $\alpha$ /RXR $\alpha$  or LXR $\alpha$ /RXR $\alpha$  heterodimers.

Intrinsic fluorescence quenching experiments provided more insight into how the protein-DNA interactions observed in EMSAs occurs. A 1:1 mixture of PPAR $\alpha$  and LXR $\alpha$  bound all three candidate REs with very high affinity, apparent  $K_d$  values of less than 5 nM. The affinity for the P4RE was slightly lower than for the L4RE or the H4RE. However, it is important to note that apparent  $K_d$  value alone is not an accurate representation of binding, as many factors may produce skewed apparent  $K_d$  values. For example, based on  $K_d$  value alone, PPAR $\alpha$  appears to exhibit high affinity binding to candidate REs, as well as to ACOX and SREBP, in the absence of a heterodimer partner. Since such a conclusion is inconsistent with data obtained from EMSA experiments, it is also necessary to consider whether the concentration dependence for oligonucleotide-induced changes in protein fluorescence exhibit hyperbolic or sigmoid shapes. In the event of high affinity binding, such a plot would present as a steep hyperbolic curve that reaches saturation far to the left on the x-axis. In the case of PPAR $\alpha$ -only samples, the curves obtained were relatively shallow, and did not appear to reach saturation within the range of concentrations tested. These data indicate that, instead of high affinity binding

suggested by estimated  $K_d$  value alone, PPAR $\alpha$  binds these candidate RE sequences, as well as ACOX and SREBP-1c, with a very low affinity or in a nonspecific manner.

This hypothesis is supported by the data for the PPAR $\alpha$ /LXR $\alpha$  mixture. The binding curves generated from these data appear to reach saturation at low concentrations of DNA, but begin climbing again towards the higher concentrations. Since the curve does not fully plateau upon reaching saturation, the presence of multiple binding sites was possible. A Hill plot showed a slope of less than 1 supported the presence of at least two binding sites, which function in a negatively cooperative manner. While uncommon among nuclear receptors, binding of RXR $\alpha$  ligand 9-cis-retinoic acid to TR/RXR heterodimers decreases the affinity of 3,3,5-tri-iodothyronine (T3) for TR, resulting in negative cooperativity within the heterodimer [52]. Additionally, it has been proposed that, along with direct binding as with a PPAR $\alpha$ /RXR $\alpha$  heterodimer, PPAR $\alpha$  may also be able to affect gene regulation indirectly. A heterodimer partner binds DNA directly while PPAR $\alpha$  binds weakly or nonspecifically [53]. Such a mechanism would explain the shape of the binding curves, with the initial saturation representing a high affinity site, presumably LXR $\alpha$ , and the subsequent increased change in intensity at higher DNA concentrations corresponding to a low affinity site representing PPAR $\alpha$ .

These data show that LXR $\alpha$ , unlike PPAR $\alpha$ , is capable of binding to DNA in the absence of a heterodimer partner. While murine LXR $\alpha$  has been shown to bind a cAMP-responsive response element (CNRE) as a monomer to regulate the renin gene, interaction with a DR4 LXRE was shown to be homodimeric [54]. To wit, binding to DNA by human LXR $\alpha$  in the form of a homodimer has not been previously

demonstrated. Shifted protein-DNA complexes were seen in LXR $\alpha$ -only EMSAs with all three candidate REs, as well as with the ACOX PPRE and SREBP-1c LXRE in previous work. Furthermore, the presence of an LXR $\alpha$ -DNA complex was suggested in supershift assays, where addition of a PPAR $\alpha$  antibody resulted in a supershift. However, a second, unshifted band was also present. In contrast, the addition of a LXR $\alpha$  antibody produced only a single supershifted band. These results could be caused by antibody affinity and epitope accessibility, but both antibodies were tested on their respective RXR $\alpha$  heterodimers, and no second complex was observed. Fluorescence quenching assays confirmed the specificity of this binding, as well as the idea that the high affinity binding observed with PPAR $\alpha$ /LXR $\alpha$  experiments was due to binding by LXR $\alpha$ . In the absence of PPAR $\alpha$ , LXR $\alpha$  demonstrated very high affinity binding to all three candidate REs as well as to ACOX and SREBP-1c. It is possible that homodimeric LXR $\alpha$  exists in cells when levels of protein and/or ligand do not favor formation of a heterodimer with RXR $\alpha$  or PPAR $\alpha$ , but such conditions are the focus of other projects in the laboratory and have yet to be elucidated.

In order to determine the functional significance of these findings, the occurrence of the three candidate RE sequences within the human genome was investigated. Exact matches from a BLAST search of the 16-nucleotide H4RE sequence were not obtained, and P4RE sequence were rare, with only a single site on chromosome 12. Results for the L4RE sequence, however, were surprisingly numerous. Around 87,000 results were obtained for the exact L4RE sequence used in the *in vitro* experiments in this study, with e-values ranging from 0.027 to 0.004, suggesting that they are not occurring simply due to chance. When compared to results from overlapped PPAR $\alpha$  and LXR $\alpha$  binding sites

determined by ChIP-seq, many incidences of the L4RE were present within close range. Since the significance of the 4 spacer nucleotides is not entirely understood, it is possible that other sites bound by either PPAR $\alpha$ /LXR $\alpha$  heterodimers or LXR $\alpha$  homodimers could be revealed with different nucleotides in those positions, for the P4RE and the H4RE in addition to the L4RE. It is also interesting to note that most of the LXR $\alpha$  sites from Feldmann et al. do not line up with the L4RE BLAST results, and do not also line up with the PPAR $\alpha$ /LXR $\alpha$  overlaps. It is possible that, since the ChIP-seq experiments from Boergesen et al. were conducted in mouse liver and those from Feldmann were done in macrophage foam cells, LXR $\alpha$ 's DNA binding activity may be tissue-specific. While PPAR $\alpha$  is present in macrophages, it is possible that LXR $\alpha$  may instead interact with the more prominent PPAR $\gamma$  in those cells. It has been previously suggested with TR, a nuclear receptor in the same superfamily as LXR $\alpha$ , that the sequence surrounding nuclear receptor response element half-sites are important for determining which proteins are necessary in order to affect gene expression [55]. Certain nucleotides immediately 5' of the AGGTCA half-site render the binding site more optimal for binding by TR as a homodimer, while others will require RXR $\alpha$  in order to bind and affect gene expression. Given the frequency of the L4RE within the human genome and the relative scarcity of binding sites observed in ChIP-seq experiments, it is possible that a similar mechanism is at work with LXR $\alpha$ .

The ability of LXR $\alpha$  to influence the expression of genes as a heterodimer with PPAR $\alpha$  or as a homodimer was tested via transactivation assays using firefly luciferase reporters and a selection of incidences of the L4RE sequence within 5 kb of an endogenous promoter. Such genomic locations were chosen to present a more focused

portrait of the consequences of homodimeric and heterodimeric DNA binding by LXR $\alpha$  compared to that of a viral promoter, such as TK or CMV. The design of the plasmids used in this study ensures that the effect seen on luciferase expression as driven by the gene promoter closely resembles that which may occur *in vivo*. Furthermore, COS-7 cells were chosen due to their low endogenous expression of PPAR $\alpha$ , LXR $\alpha$ , and RXR $\alpha$ , despite not being human-derived cells. HepG2 cells, while a human-derived cell line widely used to study these proteins, express the proteins at very high levels causing significant experimental difficulties. All of the luciferase plasmids tested increased luciferase expression significantly when LXR $\alpha$  alone was overexpressed, while only one, APOA1, showed a statistically significant increase from the vector control when both PPAR $\alpha$  and LXR $\alpha$  were overexpressed. In fact, overexpressing PPAR $\alpha$  in addition to LXR $\alpha$  resulted in an overall decrease in transactivation compared to LXR $\alpha$  alone. It is possible that some observed transactivation in cells overexpressing LXR $\alpha$  was due to the exogenous LXR $\alpha$  interacting with endogenous RXR $\alpha$ , but overexpression of RXR $\alpha$  in addition to LXR $\alpha$  did not result in a corresponding increase in transactivation, suggesting that the majority of RE activity in those cells was due to LXR $\alpha$  alone. It is important to note that, when co-overexpressed with either PPAR $\alpha$  or RXR $\alpha$ , the increase in LXR $\alpha$  expression noted in the immunoblot is not as profound as when it is overexpressed on its own. This may be the reason for this discrepancy, but is more likely to suggest a dependency on sufficient concentrations of LXR $\alpha$ . Furthermore, the presence of PPAR $\alpha$  decreased transactivation of all reporters examined. It is therefore possible that LXR $\alpha$  homodimers function to resume the activity of LXR $\alpha$ /RXR $\alpha$  heterodimers in the event of a shortage of RXR $\alpha$ , or in response to a different cellular environment, while



PPAR $\alpha$ /LXR $\alpha$  heterodimers function to counteract LXR $\alpha$  activity in some aspects while carrying it on, albeit at a lower level, in others.

These findings suggest that the role of LXR $\alpha$  in metabolic regulation needs to be included when considering clinical significance of these proteins. Although small molecule ligand effects were not within the scope of this study and when considering LXR $\alpha$  as a possible therapeutic target for metabolic disorders, understanding the mechanisms involved and pathways controlled by each form of the protein. LXR $\alpha$  as an agonist could be a powerful tool for treatment of disorders such as atherosclerosis, cardiovascular disease and hypercholesterolemia, but agonists may affect LXR $\alpha$  function differently in an environment that favors the formation of a PPAR $\alpha$ /LXR $\alpha$  heterodimer rather than an LXR $\alpha$ /RXR $\alpha$  heterodimer, which may in turn function differently in an environment favoring LXR $\alpha$  homodimer formation. In the case of SREBP-1c, which is involved in the synthesis of both cholesterol and fatty acids, LXR $\alpha$  alone was capable of transactivating the gene's endogenous promoter nearly as well as LXR $\alpha$ /RXR $\alpha$  heterodimers, while PPAR $\alpha$ /LXR $\alpha$  did not produce significant transactivation of the gene. However, PPAR $\alpha$ /LXR $\alpha$  did transactivate APOA1, although at lower levels than did LXR $\alpha$  alone or LXR $\alpha$ /RXR $\alpha$ , which plays an important role in mitigating atherosclerosis by facilitating removal of cholesterol from the body. It is possible, then, that the PPAR $\alpha$ /LXR $\alpha$  heterodimer may function to suppress LXR $\alpha$ /RXR $\alpha$  activity, presumably as well as LXR $\alpha$  homodimer activity, in the presence of high levels of cholesterol and facilitate its breakdown and elimination. It follows, then, that if PPAR $\alpha$ /LXR $\alpha$  is capable of activating other anti-atherosclerotic targets of LXR $\alpha$ , but not those involved in synthesis of fatty acids and triglycerides, and the conditions favoring

PPAR $\alpha$ /LXR $\alpha$  heterodimerization were elucidated, it may be possible to determine a means to drive cellular metabolism toward its formation as a therapeutic measure against atherosclerosis and hypercholesterolemia while avoiding adverse side effects from LXR $\alpha$ 's involvement in fatty acid synthesis.

In conclusion, the role of nuclear receptors, and LXR $\alpha$  in particular, in regulation of metabolic function is extremely complex, and involves a great deal of cross-talk and direct interaction with other proteins as it recognizes and binds target DNA sequences to affect levels of gene expression. This study demonstrated LXR $\alpha$  binding *in vitro* as both a heterodimer with PPAR $\alpha$  and, for the first time, as a homodimer, to a DR4 DNA sequence that naturally occurs in the human genome with great frequency. Furthermore, these data showed that a PPAR $\alpha$ /LXR $\alpha$  heterodimer does not bind the known PPAR $\alpha$  target in the ACOX gene, nor does it bind the LXR $\alpha$  target in SREBP-1c. Finally, the findings of this study determined that both PPAR $\alpha$ /LXR $\alpha$  heterodimers and LXR $\alpha$  homodimers are capable of transactivating endogenous promoters in cells and suggest a novel role for these forms of LXR $\alpha$  in the overall maintenance of energy homeostasis. The effects of synthetic and endogenous ligands on DNA binding and transactivation by LXR $\alpha$  homodimers and PPAR $\alpha$ /LXR $\alpha$  heterodimers, as well as that of mutant proteins that disrupt protein-protein and protein-DNA interactions, have yet to be investigated. Determination of further sequences which may be bound by LXR $\alpha$  homodimers or PPAR $\alpha$ /LXR $\alpha$  heterodimers could be accomplished using a high-throughput systematic evolution of ligands by exponential enrichment (SELEX) experimental approach [57], and would be beneficial to understanding the critical role these proteins play in energy metabolism and homeostasis.

## LIST OF ABBREVIATIONS

ABCA1 – ATP-binding cassette transporter A1

ACOX – Acyl-CoA oxidase

APOA1 – Apolipoprotein AI

ChIP – Chromatin immunoprecipitation

CYP7A1 – Cholesterol 7 $\alpha$  hydroxylase

DBD – DNA binding domain

DRx – Direct repeat

DTT – Dithiothreitol

EDTA – Ethylenediaminetetraacetic acid

EMSA – Electrophoretic mobility shift assay

ER – Estrogen receptor

FAS – Fatty acid synthase

LBD – Ligand binding domain

LXR – Liver X receptor

LXRE – Liver X receptor response element

PPAR – Peroxisome proliferator-activated receptor

PPRE – Peroxisome proliferator response element

RE – Response element

RXR – Retinoid X receptor

SELEX - Systematic Evolution of Ligands by Exponential Enrichment

SREBP – Sterol regulatory element binding protein

TR – Thyroid hormone receptor

## REFERENCES

1. Rochette-Egly, C., *Nuclear receptors: integration of multiple signaling pathways through phosphorylation*. Cell Signal, 2003. **15**(4): p. 355-66.
2. Aranda, A. and A. Pascual, *Nuclear hormone receptors and gene expression*. Physiol Rev, 2001. **81**(3): p. 1269-304
3. Oswal, D.P., G.M. Alter, S.D. Rider, Jr., and H.A. Hostetler, *A single amino acid change humanizes long-chain fatty acid binding and activation of mouse peroxisome proliferator-activated receptor  $\alpha$* . J Mol Graph Model, 2014. **51**: p. 27-36.
4. Svensson, S., T. Ostberg, M. Jacobsson, C. Norström, K. Stefansson, D. Hallén, I.C. Johansson, K. Zachrisson, D. Ogg, and L. Jendeberg, *Crystal structure of the heterodimeric complex of LXR $\alpha$  and RXR $\beta$  ligand-binding domains in a fully agonistic conformation*. EMBO J, 2003. **22**(18): p. 4625-33.
5. Singaraja, R.R., V. Bocher, E.R. James, S.M. Clee, L.H. Zhang, B.R. Leavitt, B. Tan, A. Brooks-Wilson, A. Kwok, N. Bissada, Y.Z. Yang, G. Liu, S.R. Tafuri, C. Fievet, C.L. Wellington, B. Staels, and M.R. Hayden, *Human ABCA1 BAC transgenic mice show increased high density lipoprotein cholesterol and ApoAI-dependent efflux stimulated by an internal promoter containing liver X receptor response elements in intron 1*. J Biol Chem, 2001. **276**(36): p. 33969-79

6. Issemann, I. and S. Green, *Activation of a member of the steroid hormone receptor superfamily by peroxisome proliferators*. Nature, 1990. **347**(6294): p. 645-50.
7. Thomas, M., S. Winter, B. Klumpp, M. Turpeinen, K. Klein, M. Schwab, and U.M. Zanger, *Peroxisome proliferator-activated receptor alpha, PPAR $\alpha$ , directly regulates transcription of cytochrome P450 CYP2C8*. Front Pharmacol, 2015. **6**: 261.
8. Hostetler, H.A., A.D. Petrescu, A.B. Kier, and F. Schroeder, *Peroxisome proliferator-activated receptor alpha interacts with high affinity and is conformationally responsive to endogenous ligands*. J Biol Chem, 2005. **280**(19): 18667-82.
9. Hostetler, H.A., A.L. McIntosh, B.P. Atshaves, S.M. Storey, H.R. Payne, A.B. Kier, and F. Schroeder, *L-FABP directly interacts with PPAR alpha in cultured primary hepatocytes*. Journal of Lipid Research, 2009. **50**(8): p. 1663-1675.
10. Chakravarthy M.V., I.J. Lodhi, L. Yin, R.R. Malapaka, H.E. Xu, J. Turk, and C.F. Semenkovich, *Identification of a physiologically relevant endogenous ligand for PPARalpha in liver*. Cell, 2009. **138**(3): p. 476-88.
11. Munday, M.R., and C.J. Hemingway, *The regulation of acetyl-CoA carboxylase—a potential target for the action of hypolipidemic agents*. Adv Enzyme Regul, 1999. **39**: p. 205-34.
12. Fernández-Alvarez, A., M.S. Alvarez, R. Gonzalez, C. Cucarella, J. Muntané, and M. Casado, *Human SREBP1c expression in liver is directly regulated by peroxisome proliferator-activated receptor alpha (PPARalpha)*. J Biol Chem, 2011. **286**(24): p. 21466-77.
13. Schoonjans, K., J. Peinado-Onsurbe, A.M. Lefebvre, R.A. Heyman, M. Briggs, S. Deeb, B. Staels, and J. Auwerx, *PPAR $\alpha$  and PPAR $\gamma$  activators direct a distinct tissue-specific*

- transcriptional response via a PPRE in the lipoprotein lipase gene. EMBO J, 1996. 15(19): p. 5336-48.*
14. Zhang, L.H., V.S. Kamanna, S.H. Ganji, X.M. Xiong, and M.L. Kashyap, *Pioglitazone increases apolipoprotein A-I production by directly enhancing PPRE-dependent transcription in HepG2 cells. J Lipid Res, 2010. 51(8): p. 2211-22.*
  15. Wu, P., J.M. Peters, and R.A. Harris, *Adaptive increase in pyruvate dehydrogenase kinase 4 during starvation is mediated by peroxisome proliferator-activated receptor alpha. Biochem Biophys Res Commun, 2001. 287(2): p. 391-6.*
  16. Delerive, P., K. De Bosscher, S. Besnard, W. Vanden Berghe, J. M. Peters, F.J. Gonzalez, J.C. Fruchart, A. Tedgui, G. Haegeman, and B. Staels, *Peroxisome proliferator-activated receptor alpha negatively regulates the vascular inflammatory gene response by negative cross-talk with transcription factors NF-kappaB and AP-1. J Biol Chem, 1999; 274(45): p. 32048-54*
  17. Narala V.R., R.K. Adapala, M.V. Suresh, T.G. Brock, M. Peters-Golden, and R.C. Reddy, *Leukotriene B4 is a physiologically relevant endogenous peroxisome proliferator-activated receptor-alpha agonist. J Biol Chem, 2010. 285(29): p. 22067-74.*
  18. Hostetler, H.A., A.B. Kier, and F. Schroeder, *Very-long-chain and branched-chain fatty acyl-CoAs are high affinity ligands for the peroxisome proliferator-activated receptor alpha (PPARalpha). Biochemistry, 2006. 45(24): 7669-81.*
  19. Hostetler, H.A., H. Huang, A.B. Kier, and F. Schroeder, *Glucose directly links to lipid metabolism through high affinity interaction with peroxisome proliferator-activated receptor alpha. J Biol Chem, 2008. 283(4): p. 2246-54*

20. Yoshikawa, T., H. Shimano, M. Amemiya-Kudo, N. Yahagi, A.H. Hasty, T. Matsuzaka, H. Okazaki, Y. Tamura, Y. Iizuka, K. Ohashi, J. Osuga, K. Harada, T. Gotoda, S. Kimura, S. Ishibashi, and N. Yamada, *Identification of liver X receptor-retinoid X receptor as an activator of the sterol regulatory element-binding protein 1c gene promoter*. Mol Cell Biol, 2001. **21**(9): p. 2991-3000.
21. Chinetti, G., S. Lestavel, V. Bocher, A.T. Remaley, B. Neve, I.P. Torra, E. Teissier, A. Minnich, M. Jaye, N. Duverger, H.B. Brewer, J.C. Fruchart, V. Clavey, and B. Staels, *PPAR- $\alpha$  and PPAR- $\gamma$  activators induce cholesterol removal from human macrophage foam cells through stimulation of ABCA1 pathway*. Nature Med, 2001. **7**: p. 51-58.
22. Sabol, S.L., H.B. Brewer, Jr., and S. Santamarina-Fojo, *The human ABCG1 gene: identification of LXR response elements that modulate expression in macrophages and liver*. J Lipid Res, 2005. **46**(10): p. 2151-67.
23. Repa, J.J., K.E. Berge, C. Pomajzl, J.A. Richardson, H. Hobbs, and D.J. Mangelsdorf, *Regulation of ATP-binding cassette sterol transporters ABCG5 and ABCG8 by the liver X receptors  $\alpha$  and  $\beta$* . J Biol Chem, 2002. **277**: p. 18793-800.
24. Mitro, N., P.A. Mak, L. Vargas, C. Godio, E. Hampton, V. Molteni, A. Kreuzsch, and E. Saez, *The nuclear receptor LXR is a glucose sensor*. Nature, 2007. 445(7124): p. 219-23.
25. Stender, S., R. Frikke-Schmidt, A. Anestis, D. Kardassis, A.A. Sethi, B.G. Nordestgaard, and A. Tybjærg-Hansen, *Genetic variation in liver X receptor alpha and risk of ischemic vascular disease in the general population*. Arterioscler Thromb Vasc Biol, 2011. **31**(12): p. 2990-6.

26. Legry, V., D. Cottel, J. Ferrières, G. Chinetti, T. Deroide, B. Staels, P. Amouyel, and A. Meirhaeghe, *Association between liver X receptor  $\alpha$  gene polymorphisms and risk of metabolic syndrome in French populations*. *Int J Obes*, 2008. **32**: p. 421-28.
27. Ide, T., H. Shimano, T. Yoshikawa, N. Yahagi, M. Amemiya-Kudo, T. Matsuzaka, M. Nakakuki, S. Yatoh, Y. Iizuka, S. Tomita, K. Ohashi, A. Takahashi, H. Sone, T. Gotoda, J. Osuga, S. Ishibashi, and N. Yamada, *Cross-talk between peroxisome proliferator-activated receptor (PPAR) alpha and liver X receptor (LXR) in nutritional regulation of fatty acid metabolism. II. LXRs suppress lipid degradation gene promoters through inhibition of PPAR signaling*. *Mol Endocrinol*, 2003. **17**(7): p. 1255-67.
28. Yoshikawa, T., T. Ide, H. Shimano, N. Yahagi, M. Amemiya-Kudo, T. Matsuzaka, S. Yatoh, T. Kitamine, H. Okazaki, Y. Tamura, M. Sekiya, A. Takahashi, A.H. Hasty, R. Sato, H. Sone, J. Osuga, S. Ishibashi, and N. Yamada, *Cross-talk between peroxisome proliferator-activated receptor (PPAR) alpha and liver X receptor (LXR) in nutritional regulation of fatty acid metabolism. I. PPARs suppress sterol regulatory element binding protein-1c promoter through inhibition of LXR signaling*. *Mol Endocrinol*, 2003. **17**(7): p. 1240-54.
29. Fernández-Alvarez, A., M.S. Alvarez, R. Gonzalez, C. Cucarella, J. Muntané, and M. Casado, *Human SREBP1c expression in liver is directly regulated by peroxisome proliferator-activated receptor alpha (PPARalpha)*. *J Biol Chem*, 2011. **286**(24): p. 21466-77.
30. Anderson, S.P., C. Dunn, A. Laughter, L. Yoon, C. Swanson, T. M. Stulnig, K.R. Steffensen, R.A.S Chandraratna, J.A. Gustafsson, and J.C. Corton, *Overlapping transcriptional programs regulated by the nuclear receptors peroxisome proliferator-*



- activated receptor alpha, retinoid X receptor, and liver X receptor in mouse liver. Mol Pharmacol*, 2004. **66**(6): p. 1440-52.
31. Boergesen, M., T.A. Pedersen, B. Gross, S.J. van Heeringen, D. Hagenbeek, C. Bindsbøll, S. Caron, F. Lalloyer, K.R. Steffensen, H.I. Nebb, J.A. Gustafsson, H.G. Stunnenberg, B. Staels, and S. Mandrup, *Genome-wide profiling of liver X receptor, retinoid X receptor, and peroxisome proliferator-activated receptor  $\alpha$  in mouse liver reveals extensive sharing of binding sites. Mol Cell Biol*, 2012. **32**(4): p. 852-67.
32. Gbaguidi, G.F., and L.B. Agellon, *The atypical interaction of peroxisome proliferator-activated receptor alpha with liver X receptor alpha antagonizes the stimulatory effect of their respective ligands on the murine cholesterol 7 $\alpha$ -hydroxylase gene promoter. Biochim Biophys Acta*, 2002. **1583**(2): p. 229-36.
33. Gbaguidi G.F., and L.B. Agellon, *The inhibition of the human cholesterol 7 $\alpha$ -hydroxylase gene (CYP7A1) promoter by fibrates in cultured cells is mediated via the liver x receptor alpha and peroxisome proliferator-activated receptor alpha heterodimer. Nucleic Acids Res*, 2004. **32**(3): p. 1113-21.
34. Miyata, K.S., S.E. McCaw, H.V. Patel, R.A. Rachubinski, and J.P. Capone, *The orphan nuclear hormone receptor LXR alpha interacts with the peroxisome proliferator-activated receptor and inhibits peroxisome proliferator signaling. J Biol Chem*, 1996. **271**(16): p. 9189-92.
35. Yue, L., F. Ye, C. Gui, H. Luo, J. Cai, J. Shen, K. Shen, X. Shen, and H. Jiang, *Ligand-binding regulation of LXR/RXR and LXR/PPAR heterodimerizations: SPR technology-based kinetic analysis correlated with molecular dynamics simulation. Protein Sci*, 2005. **14**(3): p. 10453-61.

36. Oswal, D.P., M. Balanarasimha, J.K. Loyer, S. Bedi, F.L. Soman, S.D. Rider, Jr., and H.A. Hostetler, *Divergence between human and murine peroxisome proliferator-activated receptor alpha ligand specificities*. J Lipid Res, 2013. **54**(9): p. 2354-65.
37. Balanarasimha, M., A.M. Davis, F.L. Soman, S.D. Rider, Jr., and H.A. Hostetler, *Ligand-regulated heterodimerization of peroxisome proliferator-activated receptor  $\alpha$  with liver X receptor  $\alpha$* . Biochemistry, 2014. **53**(16): p. 2632-43.
38. Siersbaek, R., R. Nielsen, and S. Mandrup, *PPAR $\gamma$  in adipocyte differentiation and metabolism*. FEBS letters, 2010. **584**(15): p. 3242-49.
39. Shen, Q., Y. Bai, K.C. Chang, Y. Wang, T.P. Burris, L.P. Freedman, C.C. Thompson, and S. Nagpal, *Liver X Receptor-Retinoid X Receptor (LXR-RXR) heterodimer cistrome reveals coordination of LXR and AP1 signaling in keratinocytes*. J Biol Chem 2011; **286**(16): p. 14554-63
40. Willy, P.J., K. Umesono, E.S. Ong, R.M. Evans, R.A. Heyman, and D.J. Mangelsdorf, *LXR, a nuclear receptor that defines a distinct retinoid response pathway*. Genes Dev, 1995. **9**(9): p. 1033-45.
41. Endo-Umeda, K., S. Uno, K. Fujimori, Y. Naito, K. Saito, K. Yamagishi, Y. Jeong, H. Miyachi, H. Tokiwa, S. Yamada, and M. Makishima, *Differential expression and function of alternative splicing variants of human liver X receptor  $\alpha$* . Molecular Pharmacology Fast Forward, 2012. doi: 10.1124/mol.111.07206
42. Feldmann, R., C. Fisher, V. Kodelja, S. Behrens, S. Haas, M. Vingron, B. Timmermann, A. Geikowski, and S. Sauer, *Genome-wide analysis of LXRA activation reveals new transcriptional networks in human atherosclerotic foam cells*. Nucleic Acids Res, 2013. **41**(6): p. 3518-31.

43. Papazafiri, P., K. Ogami, D.P. Ramji, A. Nicosia, P. Monaci, C. Claradas, and V.I. Zannis, *Promoter elements and factors involved in hepatic transcription of the human ApoA-I gene positive and negative regulators bind to overlapping sites.* J Biol Chem, 1991. **266**(9): p. 5790-97.
44. Wolf, I., V. Pevzner, E. Kaiser, G. Bernhardt, E. Claudio, U. Siebenlist, R. Förster, M. Lipp, *Downstream activation of a TATA-less promoter by OCT-2, Bob1, and NF-kB directs expression of the homing receptor BLR1 to mature B cells.* J Biol Chem, 1998. **273**: p. 28831-36.
45. Huuskonen, J., M. Vishnu, P. Chau, P.E. Fielding, and C.J. Fielding, *Liver X receptor inhibits the synthesis and secretion of apolipoprotein A1 by human liver-derived cells.* Biochemistry, 2006. **46**: 15068-74.
46. Fang, H.L., S.C. Strom, H. Cai, C.N. Falany, T.A. Kocarek, and M. Runge-Morris, *Regulation of human hepatic hydroxysteroid sulfotransferase gene expression by the peroxisome proliferator-activated receptor alpha transcription factor.* Mol Pharmacol, 2005; **67**(4): p. 1257-67
47. Ou, Z., M. Jiang, B. Hu, Y. Huang, M. Xu, S. Ren, S. Li, S. Liu, W. Xie, and M. Huang, *Transcriptional regulation of human hydroxysteroid sulfotransferase SULT2A1 by LXRA.* Drug Metab Dispos, 2014. **42**(10): p. 1684-89.
48. Dunn, S.E., S.S. Ousman, R.A. Sobel, L. Zuniga, S.E. Baranzini, S. Youssef, A. Crowell, J. Loh, J. Oksenberg, and L. Steinman, *Peroxisome proliferator-activated receptor (PPAR)alpha expression in T cells mediates gender differences in development of T cell-mediated autoimmunity.* J Exp Med, 2007. **204**(2): p. 321-30.

49. Jones, D.C., X. Ding, and R.A. Daynes, *Nuclear receptor peroxisome proliferator-activated receptor  $\alpha$  (PPAR $\alpha$ ) is expressed in resting murine lymphocytes: The PPAR $\alpha$  in T and B lymphocytes is both transactivation and transrepression competent.* J Biol Chem, 2002. **277**: p. 6838-45.
50. Heine, G., A. Dahten, K. Hilt, D. Ernst, M. Milovanovic, B. Hartmann, and M. Worm, *Liver X receptors control IgE expression in B cells.* J Immunol, 2009. **182**(9)a; p. 5276-82.
51. Geyeregger, R., M. Shehata, M. Zeyda, F.W. Kiefer, K.M. Stuhlmeier, E. Porpaczy, G.J. Zlabinger, U. Jäger, and T.M. Stulnig, *Liver X receptors interfere with cytokine-induced proliferation and cell survival in normal and leukemic lymphocytes.* J Leukoc Biol, 2009. **86**(5): p. 1039-48.
52. Putcha, B.D.K., E. Wright, J.S. Brunzelle, and E.J. Fernandez, *Structural basis for negative cooperativity within agonist-bound TR:RXR heterodimers.* Proc Natl Acad Sci U S A, 2012. **109**(16): p. 6084-87.
53. McMullen, P.D., S. Bhattacharya, C.G. Woods, B. Sun, K. Yarborough, S.M. Ross, M.E. Miller, M.T. McBride, E.L. LeCluyse, R.A. Clewell, and M.E. Andersen, *A map of the PPAR $\alpha$  transcription regulatory network for primary human hepatocytes.* Chem Biol Interact, 2014. **209**: p. 14-21.
54. Tamura, K., Y.E. Chen, M. Horiuchi, Q. Chen, L. Daviet, Z. Yang, M. Lopez-Illasaca, H. Mu, R.E. Pratt, and V.J. Dzau, *LXR $\alpha$  functions as a cAMP-responsive transcriptional regulator of gene expression.* Proc Natl Acad Sci U S A, 2000. **97**(15): p. 8513-18.

55. Olson, D.P., and R.J. Koenig, *5'-flanking sequences in thyroid hormone response element half-sites determine the requirement of retinoid X receptor for receptor-mediated gene expression*. J Biol Chem, 1997. **272**(15): p. 9907-14.
56. Larijani, M., A.P. Petrov, O. Kolenchenko, M. Berru, S.N. Krylov, A. Martin, *AID associates with single-stranded DNA with high affinity and a long complex half-life in a sequence-independent manner*. Mol Cell Biol, 2007. **27**(1): p. 20-30.
57. Ogawa, N., and M.D. Biggin, *High-throughput SELEX determination of DNA sequences bound by transcription factors in vitro*. Methods Mol Biol, 2012. **786**: p. 51-63